METALS PROCESSING LABORATORY
DEPARTMENT OF METALLURGY

MASSACHUSETTS INSTITUTE OF TECHNOLOGY

CAMBRIDGE, MASSACHUSETTS

THE INVESTIGATION OF THE ACTIVATED SINTERING OF TUNGSTEN POWDER

February 28, 1963

Prepared under U.S. Navy, Bureau of Naval Weapons Contract NO w 61-0326-d

FINAL REPORT
Covering the period Nov. 1, 1961 to Jan. 31, 1963

by

J. H. Brophy

H. W. Hayden

A. L. Prill

J. Wulff

Metals Processing Laboratory

Department of Metallurgy

MASSACHUSETTS INSTITUTE OF TECHNOLOGY

CAMBRIDGE, MASSACHUSETTS

ABSTRACT

Low temperature densification of tungsten can be accelerated by additions of palladium, rhodium, ruthenium, and platinum in a manner similar to that observed with nickel additions. The cause for this acceleration is an enhancement of the grain boundary diffusion process found to dominate the densification of commercially pure tungsten in the same temperature range. In contrast to the other Group VIII elements examined, iridium retards the densification of tungsten at 1100°C. An analysis of activated solid state sintering and more conventional liquid phase sintering in tungsten indicates that the two processes are similar and together comprise a general phenomenon called carrier phase sintering.

TABLE OF CONTENTS

LIST OF FIGURES

LIST OF TABLES

PREFACE TO THE FINAL REPORT ON THE INVESTIGATION OF THE ACTIVATED SINTERING OF TUNGSTEN POWDER

The report which follows contains separate accounts of the several lines of research conducted simultaneously in the program on tungsten sintering.

During the past year the primary objective of the research was a thorough study of the enhanced densification at low temperatures which occurs in tungsten with small amounts of Group VIII transition elements added. This work was a continuation of the study of nickel activated sintering of tungsten included in two previous final reports submitted to the U. S. Navy, Bureau of Naval Weapons under Contracts Numbers NOas 59-6264-c (July 8, 1960) and NOas 61-0326-c (September 25, 1961).

The results of the research found in this report have been divided into four parts, each representing a paper which has been or will shortly be submitted for publication. Part I includes the experimental observiation that additions of palladium, rhodium, ruthenium, and platinum to tungsten accelerate low

temperature sintering in a manner complimentary to the effect of nickel. The combination of these results permit a complete interpretation of the role of Group VIII elements on tungsten sintering.

Part II deals with the observation that tungsten is the only known material to sinter by a grain boundary diffusion mechanism at low temperatures, and that iridium, suitably added, actually retards the rate of densification. Part III covers the manner in which elements which form intermetallic compounds with tungsten influence its densification. Part IV analyzes and establishes the inherent similarity between low temperature "activated" sintering and the more familiar liquid phase sintering of tungsten.

PART I

THE ACTIVATED SINTERING OF TUNGSTEN WITH GROUP VIII ELEMENTS

INTRODUCTION

The mechanisms of sintering and densification of metal powders have been extensively analyzed in the past fifteen to twenty years. During this period attention has been directed toward postulating possible mass transport mechanisms and designing experiments which would unambiguously identify the dominant or "rate controlling" step in the mechanism. It is the purpose of this presentation to summarize this analytical method to date, and to apply it to the case of sintered tungsten with Group VIII elements added.

Early theories of sintering generally recognized a reduction of total surface energy and therefore surface free energy as a thermodynamic driving force for sintering.[1] Examination of microstructure and macroscopic property changes led first to the concept that plastic flow was responsible for mass transport,[2-6] but several observations of the detailed porosity changes during sintering suggested that diffusion was a more likely mechanism.[7-10]

A logically different and powerful analytical tool in sintering investigation was the model concept explored by

Kuczynski.[11] By this method the kinetics of bonding between spheres of dimensions larger than powder particles were related to various possible mass transport processes. This resulted in expressions for time dependence of neck growth of the form:

$$x \propto t^m \qquad (1)$$

The original calculations by Kuczynski recognized mass transport by viscous flow (after Frenkel[5]), evaporation - condensation from particle-pore surfaces into the neck, volume diffusion from the interior of a particle to the neck, and surface diffusion from particle-pore surface into the neck.[11] More recently, Coble has recognized the possibility of mass transport through an interparticle grain boundary, involving two possible steps: the solution of an atom, and its movement, corresponding to the phase boundary and diffusion controlled processes of chemical kinetics.[12] These additions to Kuczynski's original possibilities illustrate that the usefulness of the model concept is determined by the completeness with which potential mass transport processes can be recognized and computed.

The problem of extending neck growth measurements to the case of sintered powder compacts was facilitated by results of Kingery and Berg.[13] These investigators showed that over-all shrinkage would be observed in a real compact

only if there was a net decrease in center-to-center distance between adjacent particles. It was further shown that linear shrinkage, $\Delta L/L_o$, would vary with time in a predictable manner with various sintering mechanisms.[13,14]

The use of spherical models as analogs to the sintering of powder compacts has been strengthened by auxiliary observations in several instances. The conclusion that sintering in metals investigated to date occurs by volume self-diffusion has been verified by several experimental results. Kirkendall porosity has been observed to occur in several pure metal systems[17] and in copper-iron powder compacts.[19] Precipitates rich in a faster diffusing solute have been observed in neck regions in copper-indium alloy spheres.[20] Several instances of agreement between calculated coefficients of proportionality between shrinkage or neck growth and time serve to strengthen the model analysis technique.[18,13,16,21] The influence of grain boundaries on sintering appears to be consistent with the diffusion model of sintering.[7,8,22,23] The influence of particle size on densification is an integral part of the coefficient of proportionality between shrinkage or neck radius and time. These have also been shown to be consistent with the models as calculated.[12,24]

A GENERAL SINTERING THEORY

Table I represents a summary of neck growth and linear shrinkage relations pertinent to the present investigation. Metallic and non-metallic systems in which the various possible mechanisms have been found to be rate controlling are included.

There are no published examples in which the grain boundary mass transport path appears to be significant in solid state sintering. However, the time dependences of linear shrinkage, namely $t^{1/2}$ and $t^{1/3}$, cited from Coble's work[12] in Table I are identical with those reported by Kingery[14] for the solution-precipitation stage of liquid phase sintering. An analysis of the calculations of these two authors reveals that the models assumed are indeed quite similar. In subsequent results on liquid phase sintered systems, Kingery and co-workers have reported agreement between this model and experimental results for iron-copper,[25] tungsten carbide-cobalt and other systems.[26] These observations suggest the interesting possibility that the presence of a liquid phase during a sintering treatment selectively accelerates the "grain boundary" mass transport path. This may be due to the increased "area" of the interparticle

TABLE I

SELECTED SINTERING RELATIONS

$x \propto t^m$ $\qquad\qquad$ $\frac{\Delta L}{L_o} \propto t^n$

Mechanism	m	n	Observed Material	Reference
Viscous Flow	1/2	1	glass	13,15,16
Evaporation-Condensation	1/3	$\frac{\Delta L}{L_o} = 0$	NaCl	13
Grain boundary phase boundary control	1/4	1/2	----	12
Volume diffusion	1/5	2/5	Cu, Ag, others	11,13,17
Grain boundary diffusion control	1/6	1/3	----	12
Surface diffusion	1/7	$\frac{\Delta L}{L_o} = 0$	Ice	18

boundary path as well as modified solubilities and interfacial energies.

The concept of an alternative mass transport process assuming greater significance under alternative experimental conditions has been proposed previously. Kuczynski mentioned the possibility that smaller particle size may cause surface diffusion to dominate sintering in pure copper.[11] Similarly, it is commonly thought that the relative importance of various diffusion processes will shift from surface to grain boundary to volume as temperature increases. In the present investigation such a process change will prove to be of significance.

There are a number of examples in which the addition of foreign material leads to accelerated sintering. It has been shown that various halides, oxides, and small amounts of metallic additives lead to more rapid sintering of metals.[27-31] In the sintering of tungsten, Pirani employed six to ten weight percent nickel for the densification of tungsten in the presence of a liquid phase.[32] In order to refine the grain size of tungsten produced by liquid phase sintering with nickel, and to reduce the required sintering temperature, the nickel was diluted with copper to form the familiar "heavy alloy" compositions.[33] Considerably smaller amounts of nickel were employed to make contact materials of greater than 99 weight percent tungsten by sintering at temperatures ranging

from 1400°C to 1600°C.[34] A portion of the latter temperature range lies below the range in which a liquid phase would be expected. More recently Vacek has reported rapid densification in tungsten containing fractions of a weight percent of iron, cobalt and nickel at temperatures from 1000°C to 1300°C.[35]

RECENT DEVELOPMENTS IN NICKEL TUNGSTEN SINTERING

A comprehensive examination has been made in the Metals Processing Laboratory at M.I.T. into the fundamental mechanism behind the striking increase in tungsten sintering rates when Group VIII elements are present at temperatures so far below the equilibrium melting point of the respective alloy systems involved. This investigation has led to the concept of a "carrier phase" sintering mechanism. At present this mechanism appears to include liquid phase sintering and possibly the other types of empir- observed cases in which a modification of sintering mechanism is effected beyond that which would be expected for a pure solid component.

Typical results of early sintering in this program showed that the addition of 0.25 weight percent nickel would permit densification of 0.5 micron tungsten powder

in the temperature range 950° to 1100°C.[36,37] After thirty minutes at 1100°C a density 92 percent of theoretical was observed, and after 16 hours, the density was 98 percent. In analyzing this behavior a model of nickel-coated tungsten spheres sintering together, as shown in Figure 1, was employed. A number of paths for tungsten transport were recognized as possibilities and were employed in calculating the time dependence of linear shrinkage.[36] The resulting expression was

$$\frac{\Delta L}{L_o} = (\text{constants})\ c^p r^q t^s \qquad (2)$$

in which c = nickel content

r = particle radius

t = time

Table II represents a summary of the various postulated mass transport paths.[36] If it is assumed that each of these is potentially a rate-controlling step in sintering, the exponents indicated in Table II would describe the dependence of linear shrinkage upon the respective variables.

The initial stages of tungsten-nickel densification were followed by measuring linear shrinkage $\Delta L/L_o$, as a function of time, nickel content and particle size. At constant size and nickel content, linear shrinkage was found to vary with the square root of time. The activation

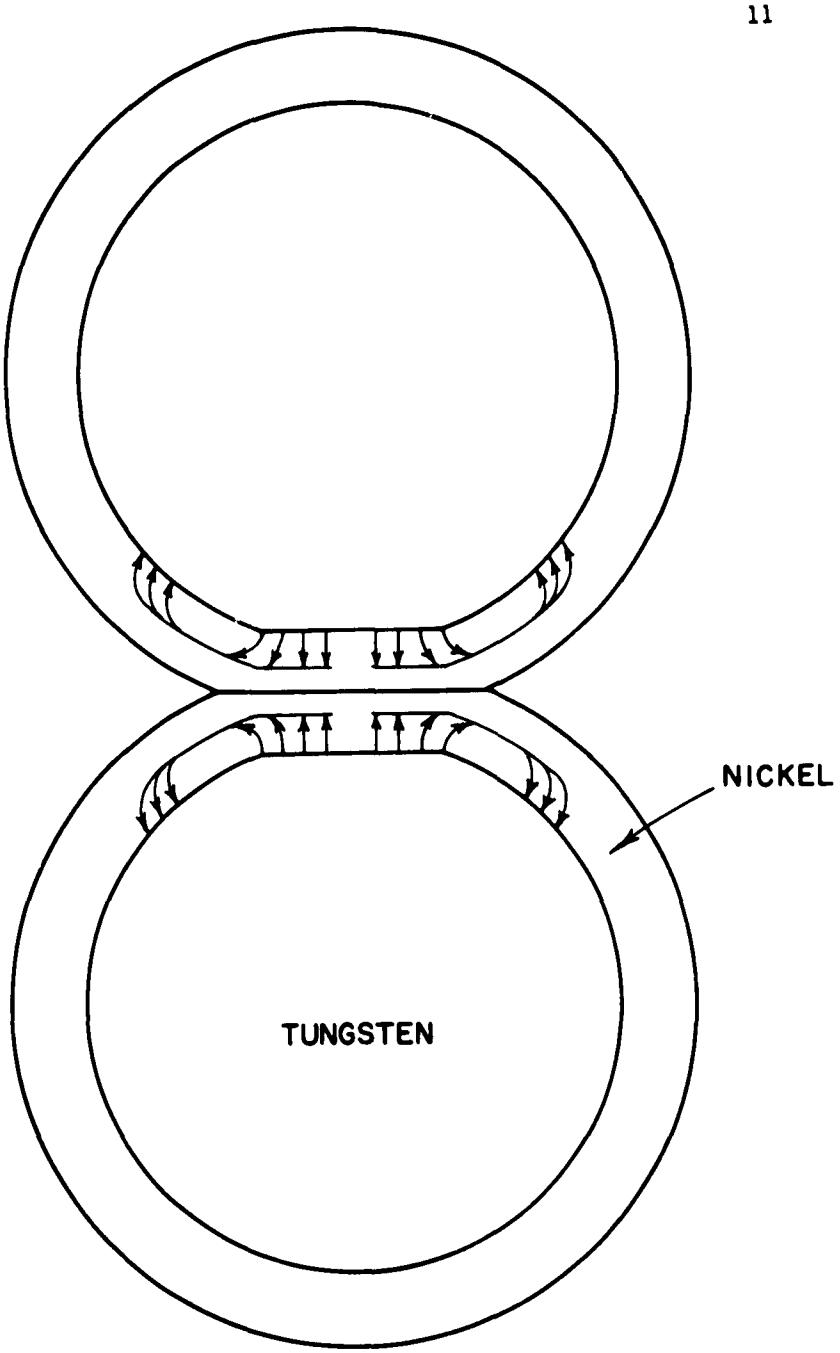

Figure 1: Schematic Representation of Sintering Nickel-Coated Tungsten Powder.

TABLE II

DENSIFICATION RELATIONS IN CARRIER PHASE SINTERING OF TUNGSTEN[36]

$$\frac{\Delta L}{L_o} = (\text{constants})\ c^p\ r^q\ t^s$$

Process	p	q	s
Tungsten solution in the carrier phase layer	0	-1	1/2
Tungsten diffusion controlled			
(1) Radially at interparticle flats	-1/2	-1	1/2
(2) Circumferentially in carrier layer	1/3	-4/3	1/3
(3) Circumferentially in interface between carrier layer and massive tungsten	0	-4/3	1/3
(4) Radially over entire particle surface	-1/3	-1	1/3

energy was 68,000 cal/mol. At constant time and particle size, linear shrinkage was found to be independent of nickel content above 0.125 weight percent. It is perhaps coincidental that this amount of nickel would be just sufficient to form a monolayer on tungsten of the particle size employed. Since all particle sizes were measured by the BET method, the correlation of linear shrinkage with particle radius at constant composition and time was not conclusive, but did show a definite decrease with increasing size. It was concluded that nickel-tungsten linear shrinkage was characterized by dependence upon the square root of time and independence of nickel content beyond a monatomic layer. Table II reveals that this behavior is typical of a process whose rate is controlled by the separation of tungsten from the particle into the nickel-rich layer. It should be noted that this process exhibits the same time dependence as the phase boundary reaction controlled processes postulated for solid state grain boundary transport[12] and liquid phase sintering.[14] On this basis it was concluded that the mechanism of nickel tungsten sintering was a kinetic intermediate between solid and liquid phase sintering.[36]

The final stage of densification in nickel-tungsten compacts was accompanied by grain growth. In more recent

work it was shown that the rate of densification was still indicative of control by "solution" of tungsten into a nickel-rich grain boundary layer.[38] The evidence for nickel remaining on the surface of tungsten particles during the early stage of sintering and at grain boundaries during the final stage is based on several experimental observations. During the final stage, grain size after a given sintering treatment was inversely proportional to the square root of nickel content, indicating that diffusion of tungsten across a nickel layer is a barrier to grain growth.[38] If nickel had been lost into the tungsten grain, the grain size should have been considerably larger than was found experimentally at lower nickel contents. Since nickel was located at the grain boundary late in the process, it must have been there from the start. In this way nickel continued to serve as an activating agent to promote densification after prolonged sintering times.

In more recent work,[39] co-reduction of nickel nitrate and tungstic oxide was employed to produce a "doped" powder. In general more nickel was required to reach comparable density in the doped powder than in the coated powder at nickel contents from 0.125 to 1.0 weight percent,

while the opposite was true at higher nickel content. This was interpreted to indicate that the distribution of a small amount of nickel was more efficient in the coated case, presumably because of its surface location.[39] In this same work, it was found that the mechanical strength of sintered nickel tungsten varied in a manner consistent with the proposed sintering model.

The experimental results indicated that nickel remained at tungsten particle surfaces and grain boundaries, probably due to low solubility and low diffusivity of nickel in tungsten at the temperatures involved. To check this possibility an approximate diffusion calculation has been made. The diffusion coefficient for nickel volume diffusion into tungsten is not available. However, using a typical D_o value ranging from 1.0 to 100.0 cm^2/gm and a Q value of 135 kcal/mole, the depth at which nickel content would be 0.001 of the surface nickel solubility has been calculated to lie between 4 and 40 $\mathring{A}$ after sintering 100 hours at 1100°C. Since the tungsten grain size after such a treatment is 50 microns and the nickel solubility in tungsten is at the most 0.3 weight percent, it appears that nickel volume diffusion into tungsten is probably negligible. At the same time, chemical analysis

revealed no total nickel loss during the sintering treatment. These two observations support the conclusion that nickel must remain at tungsten grain boundaries as indicated by the analysis of experimental sintering data.

At this point a number of issues remained unsettled in the analysis of carrier phase sintering. It was the purpose of the investigation described in the following sections to examine the kinetics of tungsten sintering in the presence of the chemical relatives of nickel in group VIII of the periodic table. The primary objectives were a description of the over-all mass transport process beyond the solution step dominating the behavior of nickel tungsten and insight into the characteristics required of an element to serve as an "activator" for tungsten diffusion and sintering.

EXPERIMENTAL PROCEDURE

The tungsten employed in this investigation was hydrogen-reduced powder of 0.56 micron BET average particle diameter purchased from the Wah Chang Corporation. Nickel was obtained in the form of reagent grade nitrate.

Palladium, rhodium, ruthenium, and platinum as chlorides were supplied initially through the courtesy of the International Nickel Company and purchased subsequently from Engelhardt Industries.

The activator compounds were weighed to yield the desired amount of the element, were dissolved in water, and mixed with the necessary amount of tungsten powder. After overnight evaporation in air at 150°C, the resulting powder cake was broken manually and pre-reduced in hydrogen at 800°C for one hour. Rectangular specimens two inches by 1/8 inch by 1/8 inch were pressed in an unlubricated steel die at 26,000 psi. Each specimen was weighted and measured in linear dimensions.

Sintering was accomplished by rapidly inserting an alundum boat containing the sample into a wire-wound vycor tube furnace at the desired temperature. After the required sintering time, the sample was similarly withdrawn from the furnace and cooled to room temperature. At all times the sample was under pre-purified hydrogen when above room temperature. It was found that about one minute was needed for each sample to reach furnace temperature, and, after sintering, about one minute passed for the sample to cool to 600°C. These intervals were recognized when

reporting sintering times.

After sintering, linear dimensions were again recorded and occasional density measurements were made. It was found that completely reproducible results were obtained using either individual samples for each sintering condition, or accumulated sintering times on a continuous sample. The latter technique was used in the bulk of the cases.

EXPERIMENTAL RESULTS AND DISCUSSION

The previous analysis of nickel-tungsten sintering employed linear shrinkage as a function of time and nickel content with particle size and temperature as parameters.[36] The postulate of solution or phase boundary control was based upon a time exponent of 1/2 and independence of nickel content combined with the data of Table II. This general technique served as an analytical outline for the data of this investigation.

Palladium-tungsten compacts were sintered at temperatures ranging from 850° to 1100°C. The time dependence of linear shrinkage is shown in Figure 2 and the composition dependence in Figure 3. The density of samples sintered 30 minutes

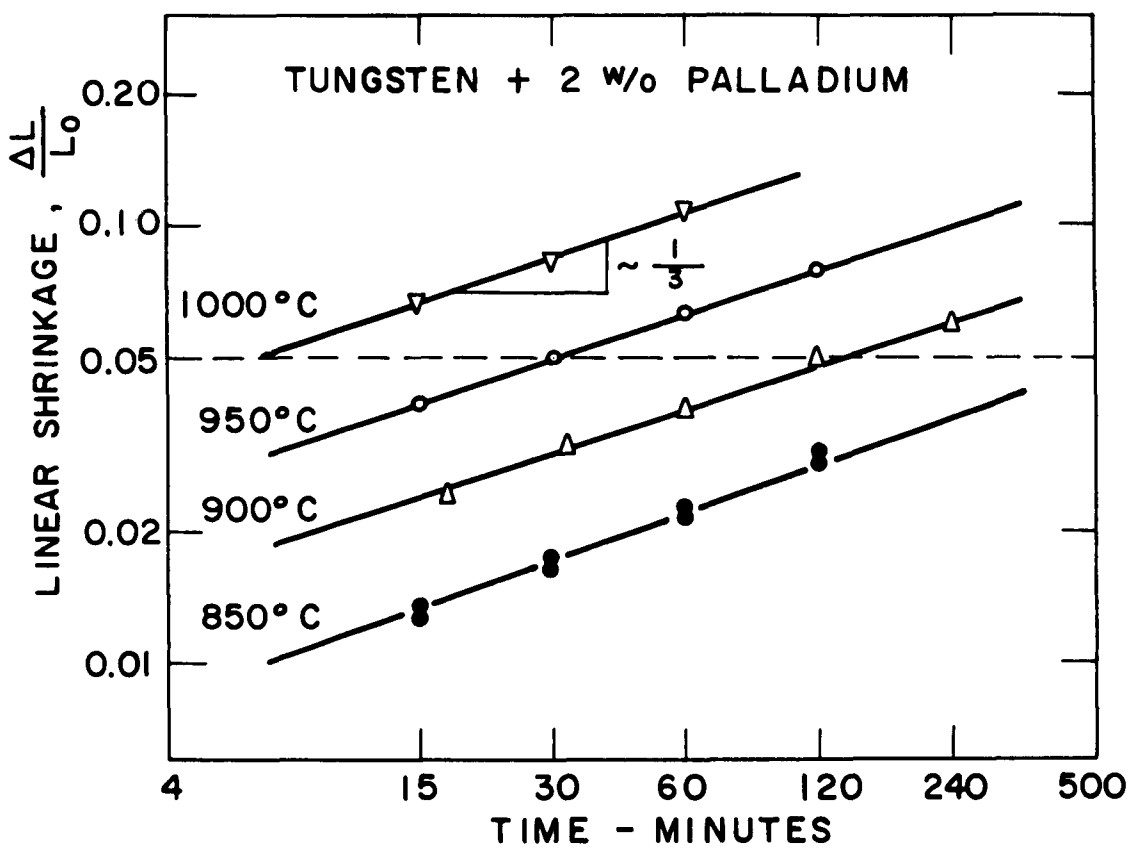

Figure 2: Time Dependence of Linear Shrinkage for Tungsten-Palladium Compacts.

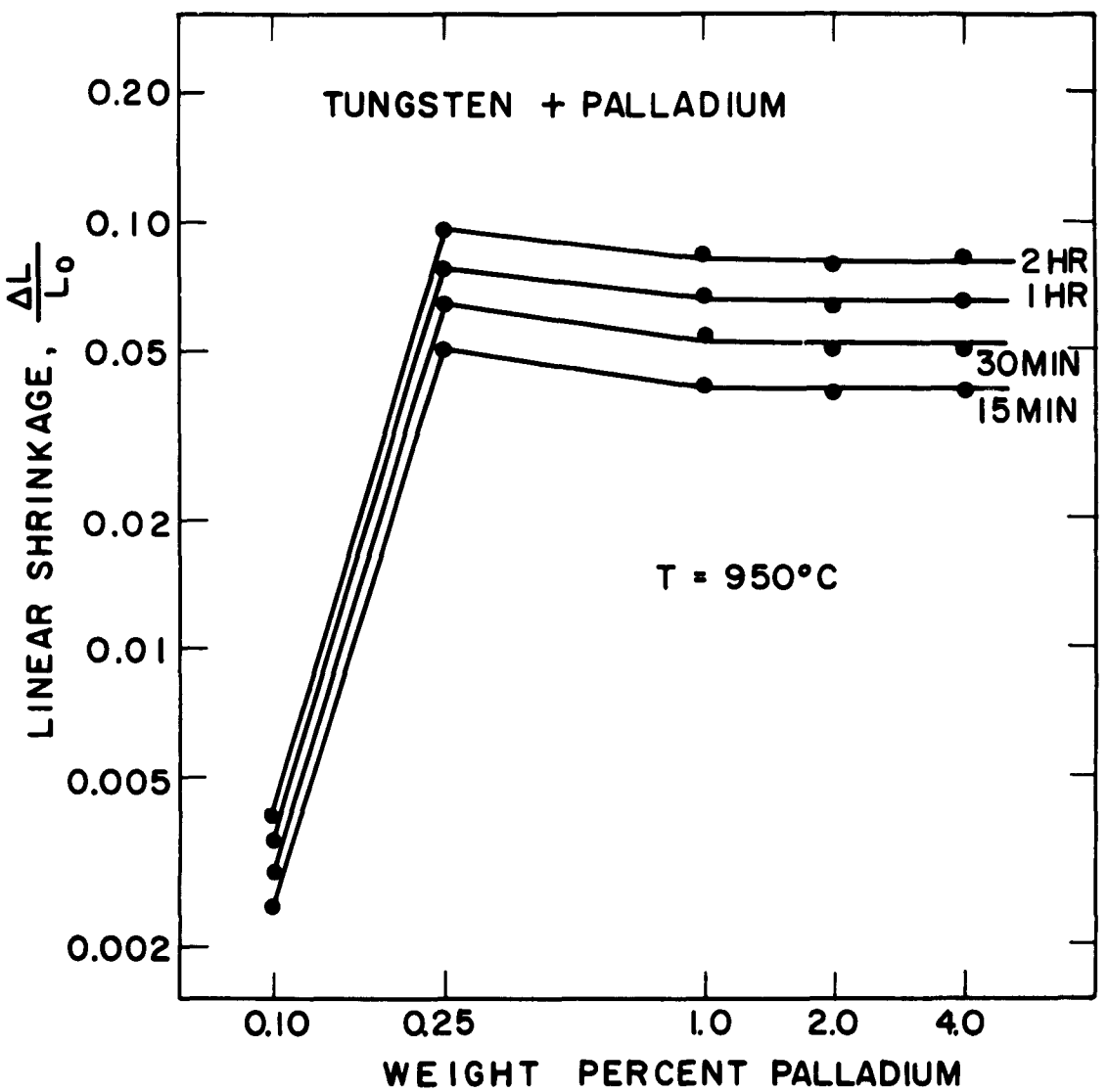

Figure 3: Composition Dependence of Linear Shrinkage for Tungsten-Palladium Compacts.

and 16 hours at 1100°C was 93.5 and 99.5 percent respectively. A comparison to the nickel-tungsten results of 92 and 98 percent shows that palladium actually caused more rapid densification than did nickel with tungsten. From Figures 2 and 3 it has been concluded that palladium-tungsten linear shrinkage depends upon the cube root of time and is essentially independent of palladium content in the range from 0.25 to 4.0 weight percent. Reference to Table II suggests that this is indicative of a transport process controlled by tungsten diffusion circumferentially in the interface between the palladium-rich layer and massive tungsten. The apparent activation energy computed from Figure 2 was 86,000 cal/mol.

Ruthenium-tungsten compacts were sintered in the temperature range 950° to 1100°C. Figure 4 shows the time dependence and Figure 5 shows the composition dependence of linear shrinkage. The slope of the curves in Figure 4 is .39, indicating that linear shrinkage varies with time to a power slightly greater than 1/3. This behavior was independent of ruthenium content above 0.5 percent. The activation energy computed from Figure 4 was 114,000 cal/mol.

Platinum-tungsten compacts were sintered at temperatures from 1000°C to 1150°C. Figure 6 shows that linear shrinkage

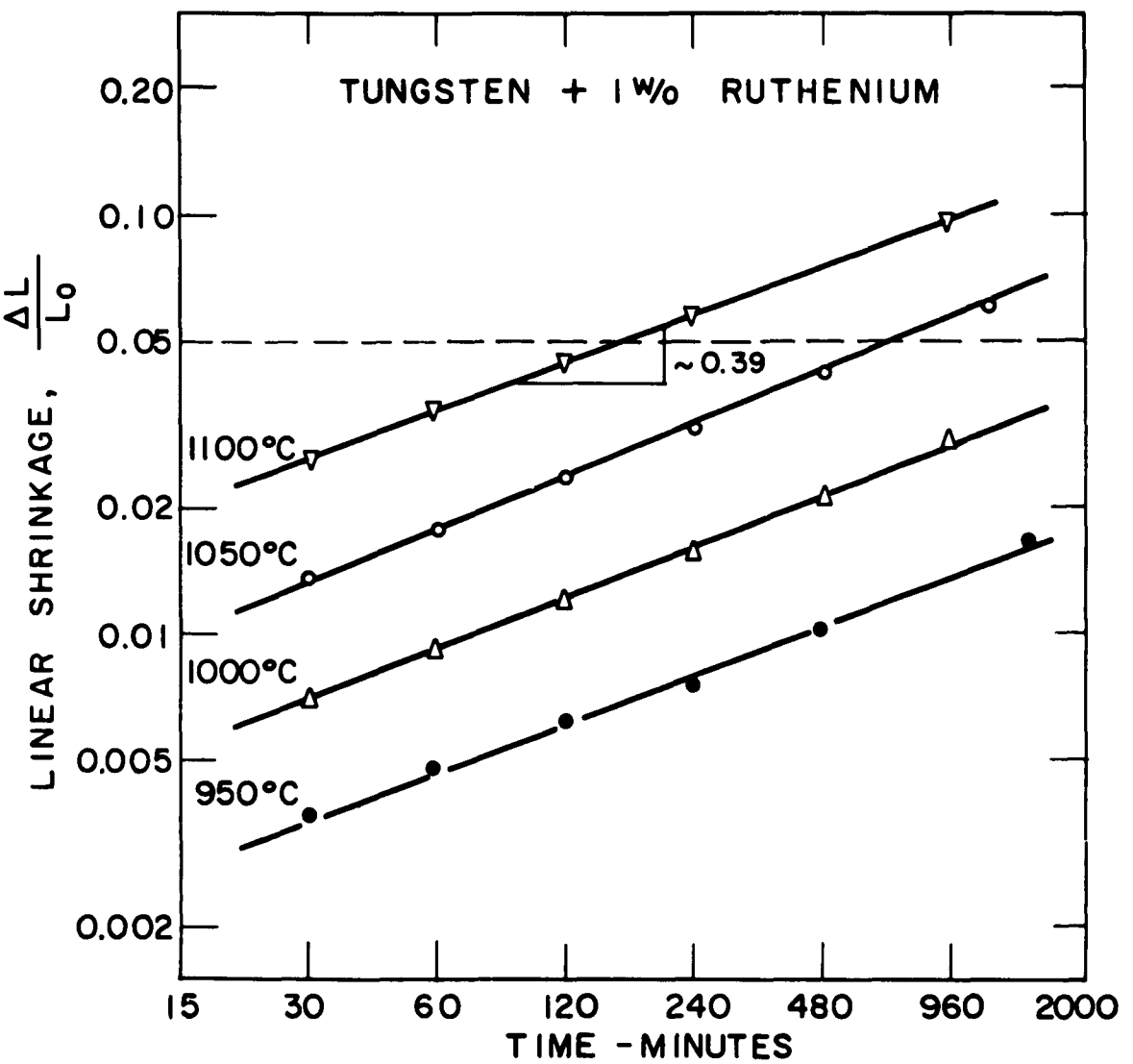

Figure 4: Time Dependence of Linear Shrinkage for Tungsten-Ruthenium Compacts.

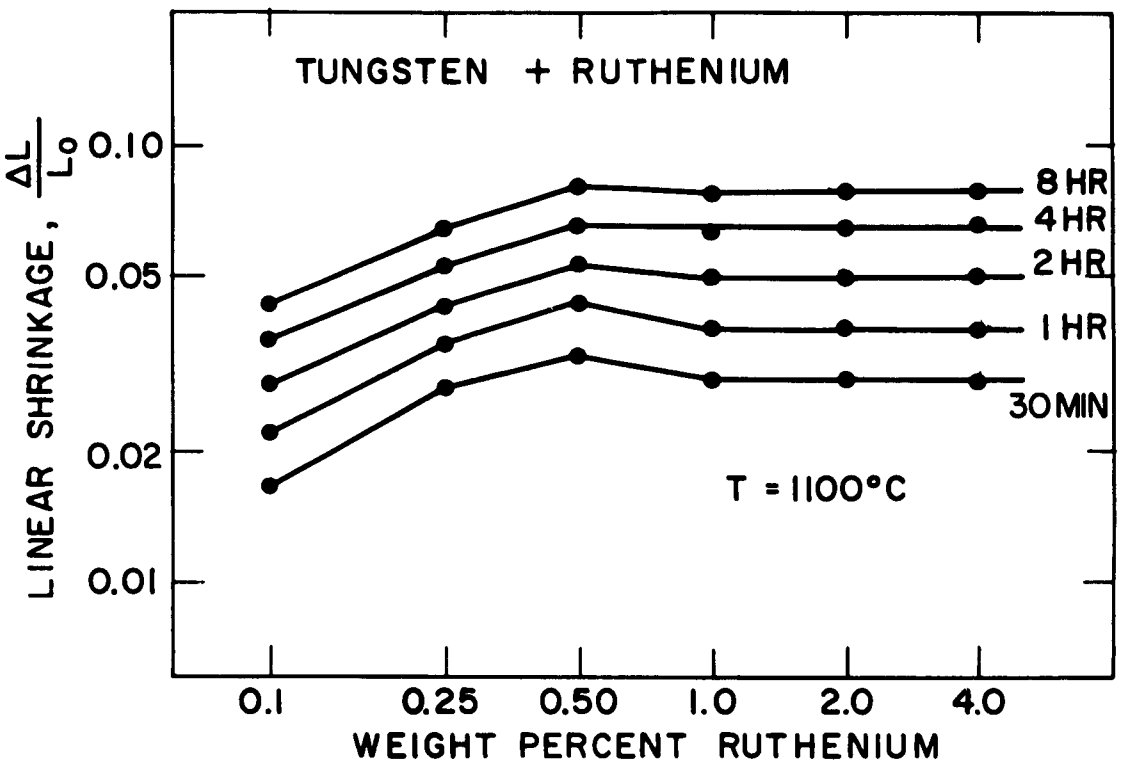

Figure 5: Composition Dependence of Linear Shrinkage Tungsten-Ruthenium Compacts.

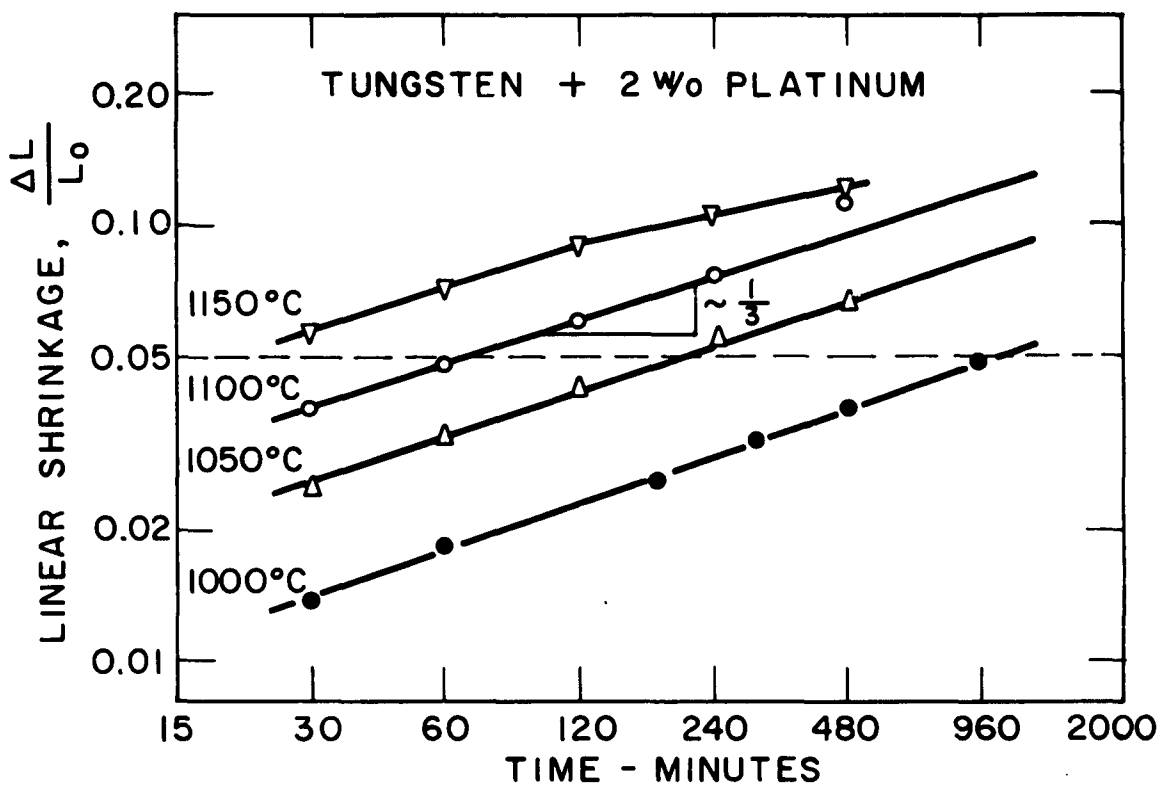

Figure 6: Time Dependence of Linear Shrinkage for Platinum-Tungsten Compacts.

varies with the cube root of time with an activation energy of 92,000 cal/mol. Figure 7 shows that linear shrinkage is independent of platinum control beyond 0.5 weight percent (approximately a monolayer). On the basis of these observations it has been concluded that platinum-tungsten sintering is controlled by the interface diffusion process.

The preceding four cases were apparently controlled either by the solution step or interface diffusion step in the tungsten transport process. With a single added element, the rate controlling step was the same over the entire range of sintering conditions employed. In the two alloy systems which follow, the rate controlling step apparently changed with sintering temperature in one case, and with amount of shrinkage in the other.

Recent results on the linear shrinkage of molybdenum sintered with nickel indicated dependence upon square root of time at 950°C and cube root at 1000° and 1100°C.[40] These results were independent of nickel content from 0.25 to 4.0 weight percent. The activation energy at temperatures between 1000° and 1100°C was 77,000 cal/mol. For this case it appears that the solution step is rate controlling at low temperatures, while interface diffusion prevails at higher temperatures.

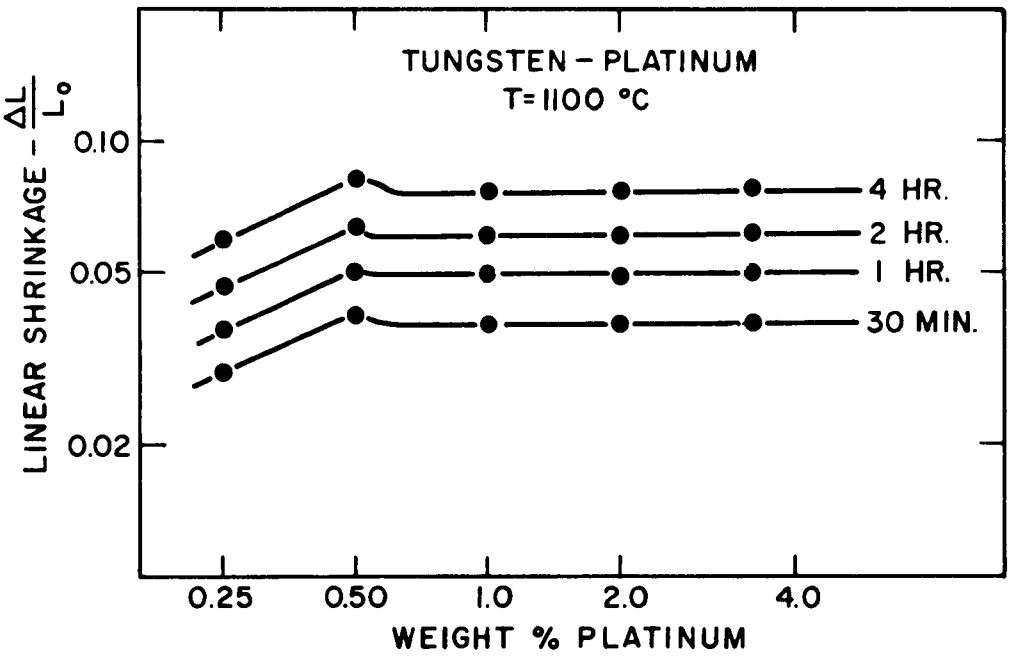

Figure 7: Composition Dependence of Linear Shrinkage for Platinum-Tungsten Compacts.

Rhodium-tungsten compacts were sintered at temperatures from 950°C to 1100°C. Figure 8 shows the time dependence of linear shrinkage. At all temperatures, the initial slope of the curve is 1/2. At higher values of linear shrinkage the slopes of the curves shift toward 1/3. Figure 9 shows that shrinkage is independent of rhodium content above 0.25 weight percent (approximately a monolayer). This behavior is consistent with a process in which the solution step controls the rate when linear shrinkage (and interparticle flat area) is small, and interface diffusion controls when shrinkage (and diffusion distance) is large.

Table III summarizes the experimental results discussed in the previous paragraphs. Figure 10 shows a compilation of Arrhenius' plots for tungsten sintering with small additions of group VIII transition elements. These curves were determined by plotting the logarithm of time necessary for five percent linear shrinkage versus the reciprocal of the absolute sintering temperature. The change in slope of the nickel tungsten curve is due to the presence of intermetallic compound at temperatures below approximately 950°C. The apparent activation energies included in Table III were obtained from Figure 10. The values for the grain

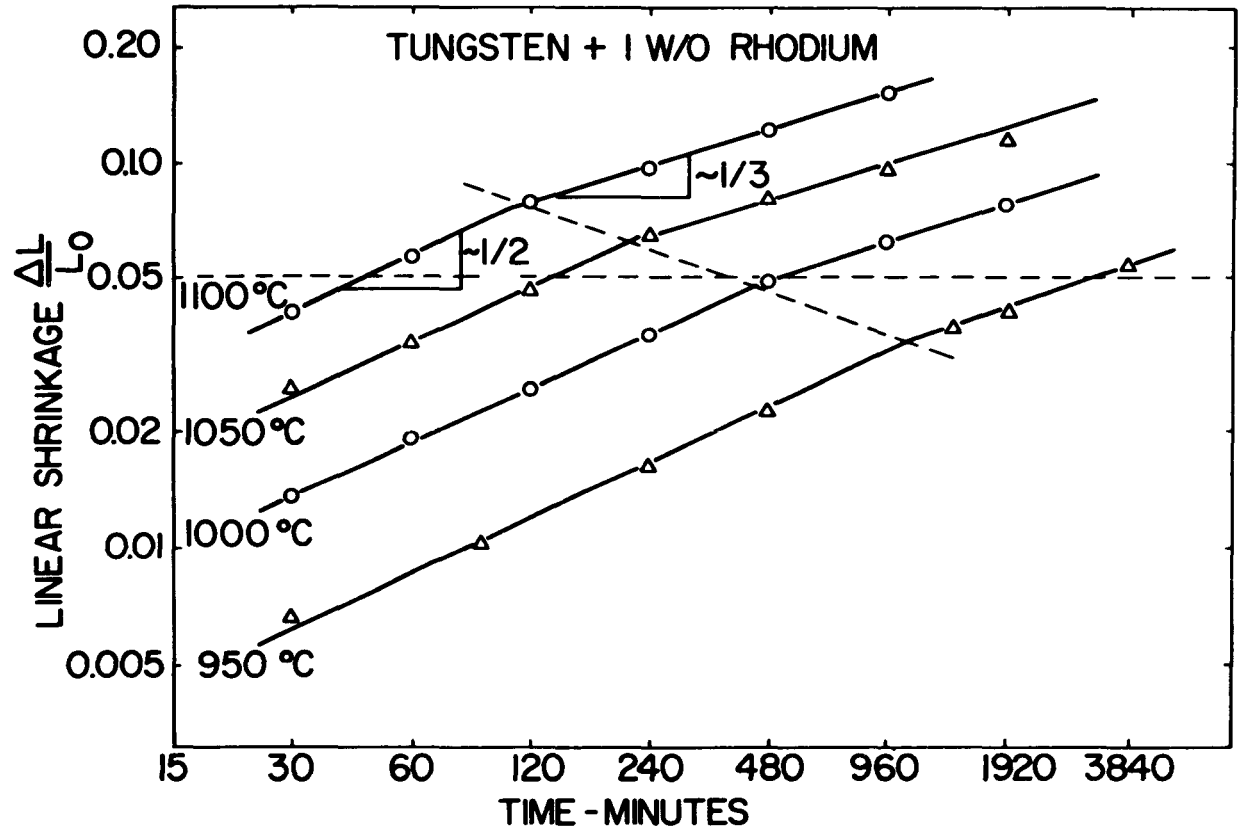

Figure 8: Time Dependence of Linear Shrinkage for Rhodium-Tungsten Compacts.

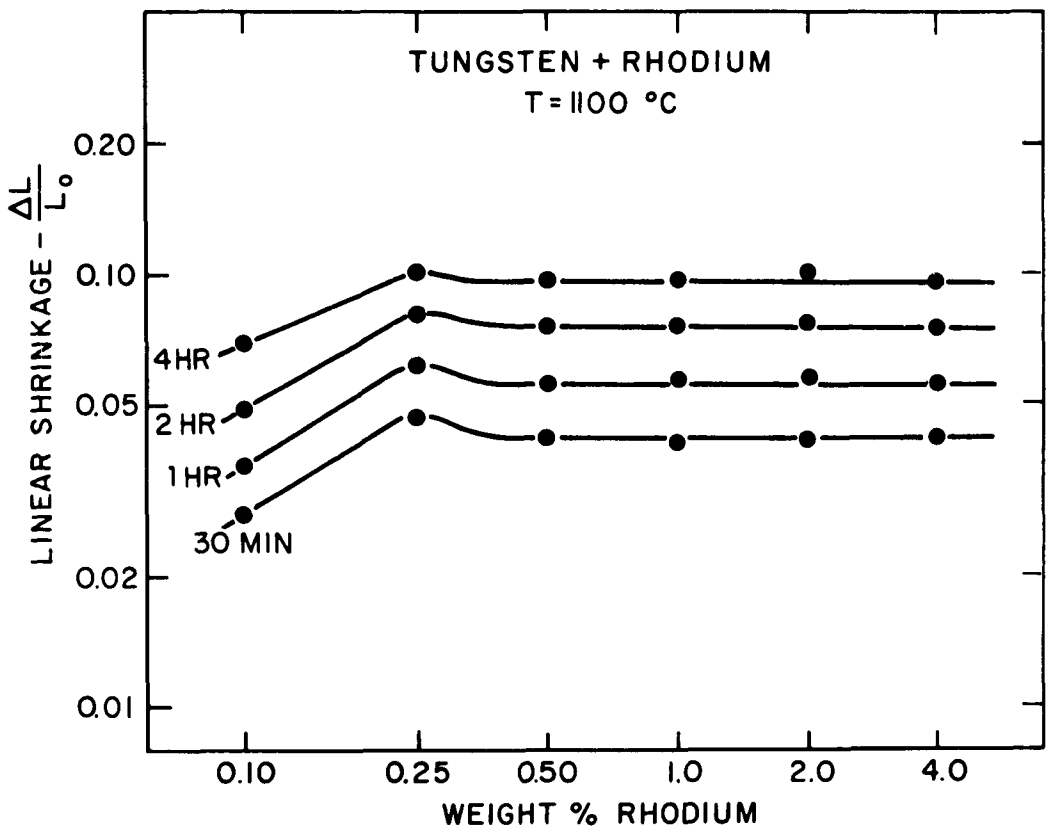

Figure 9: Composition Dependence of Linear Shrinkage for Rhodium-Tungsten Compacts.

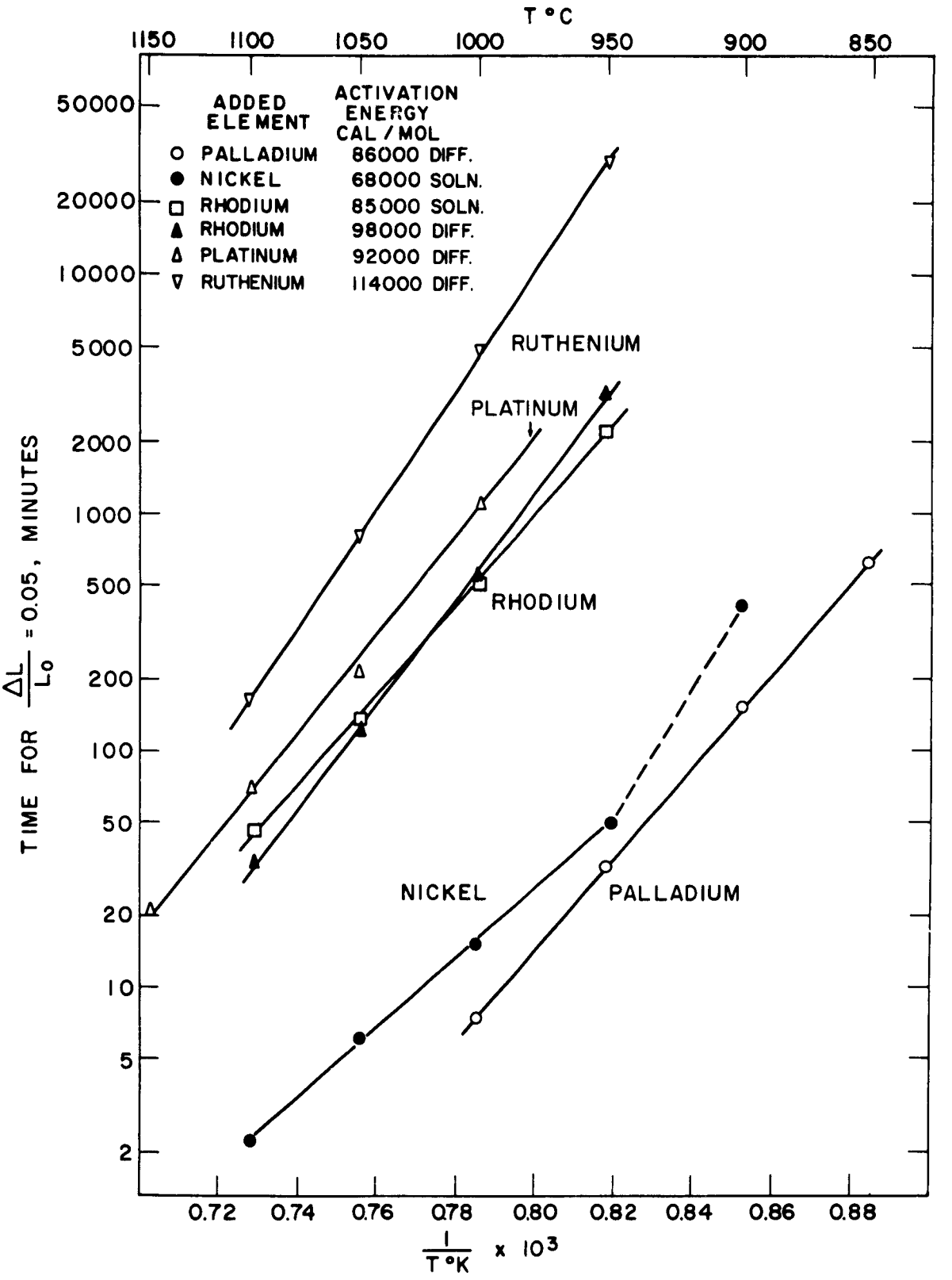

Figure 10: Arrhenius Plots of Data from Sintering of Tungsten with Additions of Palladium, Nickel, Rhodium, Platinum and Ruthenium.

TABLE III

SUMMARY OF CARRIER PHASE SINTERING RESULTS

WITH TUNGSTEN AND MOLYBDENUM

$$\frac{\Delta L}{L_o} \propto c^p t^s$$

System	p	s	Control	Activation Energy: cal/mol	Reference
W-Ni	0	1/2	Solution	68,000	36
W-Pd	0	1/3	Solution	86,000	
W-Ru	0	1/3	Diffusion	114,000	
W-Pt	0	1/3	Diffusion	92,000	
Mo-Ni					
low temp.	---	1/2	Solution	-----	40
high temp.	0	1/3	Diffusion	77,000	
W-Rh					
low shrinkage	0	1/2	Solution	85,000	
high shrinkage	0	1/3	Diffusion	98,000	

boundary diffusion path lie in the range 86,000 to 114,000 calories per mole. These values straddle the published activation energy, 90,000 calories per mole, for grain boundary diffusion of thorium in tungsten,[41] which is believed to be comparable to the activation energy for grain boundary self-diffusion in tungsten. Consequently the influence of the group VIII element is largely to increase the number of active sites for grain boundary tungsten transport.

The activation energies for the solution controlled processes with nickel and rhodium on tungsten are in general lower than those observed for diffusion control.

Figure 10 also permits a comparison of the relative effectiveness of each of the added elements in enhancing the densification of tungsten, assuming that the independence of composition observed with nickel, palladium, and ruthenium also applies to rhodium and platinum. At a given temperature, palladium led to the most rapid densification, followed in order by nickel, rhodium, platinum, and ruthenium.

The results of this investigation and of previously published work suggest a possible mechanism for what has previously been called "activated sintering" of tungsten. It appears that tungsten atoms move by a sequence of steps: first separation from the tungsten particle by a "solution"

process and, second by diffusion in the interface between the "activating" element and the tungsten particle. Both of these steps occur in series and under a given set of conditions the slower of the two determines the rate of sintering. Whether the solution step or diffusion step controls the rate, depends on the identity of the activating element, and in some cases is determined by increasing transport path length through densification, or by the differing influence of temperature on the rates of the two steps. In either step the over-all driving force is the reduction of surface free energy, which increases the tungsten activity in the carrier phase interface at the points of particle contact.

The reason that group VIII transition elements are particularly effective as activators in tungsten sintering has not been established as yet. It may prove to be associated with the fact that they all dissolve ten to twenty percent tungsten but are soluble in tungsten only to a very limited extent at the temperature employed in sintering. The fuller implications of this factor remain to be studied.

CONCLUSIONS

The densification rate in sintering tungsten powder can be significantly increased by small additions of group VIII transition elements. Of the added elements explored to date, palladium appears to have the greatest effect, followed in order by nickel, rhodium, platinum and ruthenium. With 9.25 weight percent palladium densities of 93.5 and 99.5 percent of theoretical were obtained after sintering thirty minutes and sixteen hours, respectively, at 1100°C.

A mechanism for this increased densification rate has been proposed. The activating element appears on the tungsten particle surface forming a "carrier phase" layer. Tungsten dissolves preferentially into the layer at points of particle contact and diffuses outward in the interface between the carrier phase layer and the particle itself. The result is a decrease in distance between adjacent particle centers and over-all shrinkage of the powder compact. The rate of the process is significant at temperatures well below the minimum melting points in the binary alloy systems between the added elements and tungsten, and below the temperatures ordinarily required to sinter tungsten powder of commercial purity.

The carrier phase sintering process is an example of

the selective acceleration of one of the possible mass transport mechanisms previously proposed for sintering pure solid components. This analysis suggests that liquid phase sintering, formerly considered to be distinct from sintering in the solid state, is one of the special cases of carrier phase sintering. Under a given set of experimental conditions one of the mass transport processes may be observed to control sintering rate of a pure component. The identity of the rate controlling process may change with changing experimental conditions. This has been demonstrated with changing particle size, and sintering temperature, and with the presence of foreign phases which are gaseous, liquid, or solid.

REFERENCES

1. C. Herring, "Surface Tension as a Motivation for Sintering," Phys. of Powd. Met., ed. by W.E. Kingston, McGraw-Hill, New York (1951) p. 143.

2. P. W. Clark, J. White, "Some Aspects of Sintering," Trans. Brit. Cer. Soc., 49 (1950) p. 305.

3. J. K. Mackenzie, R. Shuttleworth, "A Phenomenological Theory of Sintering," Proc. Phys. Soc., (London) B62 (1949) p. 833.

4. J. Frenkel, Jour. Phys. USSR, 9 (1945) p. 385.

5. A. J. Shaler, "Kinetics of Sintering Seminar", Trans. AIME 185, (1949) p. 796.

6. W. E. Kingston, G. F. Huettig, "Fundamental Problems of Sintering Processes," Phys. of Powd. Met., ed. by W. E. Kingston, McGraw-Hill, New York (1951) p. 1.

7. F. N. Rhines, C. E. Birchenall, L. A. Hughes, "Behavior of Pores during Sintering of Copper Compacts", Trans. AIME, 188 (1950) p. 378. (Also Rhines in discussion of "5" above)

8. B. H. Alexander, R. W. Balluffi, "Experiments on Mechanism of Sintering", J. Met. (Oct. 1950) p. 1219 (tech. note). BHA and RWB, "Mech. of Sintering of Copper", Acta Met., 5 (1957) p. 666.

9. C. Herring, "Diffusional Viscosities of a Polycrystalline Solid", J. App. Phys., 21 (1950) p. 437.

10. F. R. N. Nabarro, "Deformation of Crystals by Motion of Single Ions", Rep. on Conf. on Strength of Solids, Phys. Soc. London (1948) p. 75.

11. G. C. Kuczynski, "Self Diffusion Sintering of Metallic Particles", Trans. AIME 185 (1949) 169.

12. R. L. Coble, "Initial Sintering of Alumina and Hematite", J. Amer. Cer. Soc. 41 No. 2 (1958) p. 55.
Also: R. L. Coble, "Diffusion Sintering in Solid State", Kinetics of High Temperature Processes, W. D. Kingery (ed), Tech. Press-Wiley (1959) p. 147.

13. W. D. Kingery, M. Berg, "Study of Initial Stages of Sintering Solids by Viscous Flow, Evap-Cond, and Self Diffusion", J. App. Phys. 26 (1955) p. 1205.

14. W. D. Kingery, "Densification during Sintering in Presence of a Liquid Phase", I. Theory, J. App. Phys., 30 (1959) No. 3, p. 301.

15. G. C. Kuczynski, "Study of Sintering of Glass", J. App. Phys., 20 (1949) p. 1160.

16. G. C. Kuczynski, J. Zapiatynski, "Sintering of Glass", J. Amer. Ceramic Soc., 39 No. 10 (Oct. 1956) p. 349.

17. G. C. Kuczynski, B. M. Alexander, "Metallographic Study of Diffusion Interfaces", J. App. Phys., 22 (1951) p. 344.

18. W. D. Kingery, "Regelation, Surface Diffusion and Ice Sintering", J. App. Phys. 31 (1960) p. 833.

19. G. Matsumura, "Swelling of Iron Copper Compact during Sintering", Planseeberichte fur Pulvermetallurgie, 9 (1961) p. 33.

20. G. C. Kuczynski, G. Matsumura, B. D. Cullity, "Segregation in Homogeneous Alloys during Sintering", Acta Met. 8 (March 1960) p. 209.

21. G. C. Kuczynski, "Measurement of Self Diffusion of Silver without Radio-active Tracers," J. App. Phys., 21 (1950) p. 632.

22. J. E. Burke, "Role of Grain Boundaries in Sintering," J. Amer. Cer. Soc., 40 (March 1957) No. 3 p. 80.

23. L. Seigle, "Role of Grain Boundaries in Sintering," W. D. Kingery, Kinetics of High Temperature Processes, Tech. Press-Wiley, (1959) p. 172.

24. C. Herring, "Effect of Change of Scale on Sintering Phenomena," J. App. Phys. 21 (1950) p. 301.

25. W. D. Kingery, M. D. Narasimhan, "Densification during Sintering in Presence of Liquid Phase," II Experiment, J. App. Phys. 30 (1959) No. 3 p. 307.

26. W. D. Kingery, E. Niki, M. D. Narasimhan, "Sintering of Oxide and Metal Composite in the Presence of a Liquid Phase," J. Amer. Cer. Soc., 44 (1961) p. 29.

27. M. Eudier, "Activated Sintering," Thirteenth Annual M.P.A. Proceedings (1957) p. 5.

28. D. J. Jones, "Practical Aspects of Sintering Tungsten and Molybdenum," J. Less Common Metals, 2 (1960) p. 76.

29. W. D. Jones, Fundamental Principles of Powder Metallurgy, St. Martin's New York (1961) p. 402.

30. W. H. Lenz, J. M. Taub, "Liquid Oxide Phase Sintering of Mo and W." J. Less Common Metals 3 (Oct. 1961) p. 429.

31. R. D. Hall, J. H. Ramage, "Consolidation of Metal Powders," U.S.P. 2, 431, 690 (Dec. 2) 1947.

32. M. Pirani, "Early Days of Nickel-Tungsten Powder Metallurgy," J. Electrochemical Soc., 85 (1944) p. 163.

33. G. H. S. Price, C. J. Smithells, S. V. Williams, "Sintered Alloys, Part 1-Copper-Nickel-Tungsten Alloys Sintered with a Liquid Phase Present", J. Inst. of Metals, 62 (1938) p. 239.

34. F. H. Driggs, W. H. Lenz, "Contact Alloys," U.S.P. 2, 227, 446 (Feb. 13, 1939).

35. J. Vacek, "On Influencing the Sintering Behavior of Tungsten," Planseeberichte fur Pulvermetallurgie, 7 (1959) p. 6.

36. J. H. Brophy, L. A. Shepard, J. Wulff, "Nickel Activated Sintered of Tungsten," Powder Metallurgy, ed. W. Leszynski, AIME, MPI, Interscience, New York (1961) p. 113.

37. H. W. Hayden, "Nickel Activated Sintering of Tungsten," B. S. Thesis, Metallurgy Department, M.I.T., 1960.

38. J. H. Brophy, H. W. Hayden, J. Wulff, "Final Stages of Densification of Nickel-Tungsten Compacts," Trans. AIME, 224 (1962), p. 797.

39. J. H. Brophy, H. W. Hayden, J. Wulff, "Sintering and Strength of Coated and Co-reduced Nickel-Tungsten Powder," Trans. AIME, 221 (Dec. 1961) p. 1225.

40. J. R. Buta, "The Sintering of Nickel Activated Molybdenum," S. B. Thesis, Mechanical Engineering Department, M.I.T., 1962.

41. I. Langmuir, "Thoriated Tungsten Filaments," J. Franklin Institute, 217 1934, p. 543.

Part II

Grain Boundary Diffusion in Tungsten Sintering

INTRODUCTION

In the commerical production of tungsten articles from powder, a sintering treatment at temperatures in excess of 2600°C is normally used to achieve appreciable densification. Prior to this treatment, tungsten is pre-sintered at 1000 to 1200°C to increase its strength for handling. During the pre-sintering operation, the amounts of densification observed are small unless certain added elements are present in the tungsten.(1) Recent experimental results indicate that most of the Group VIII transition elements accelerate tungsten densification in the temperature range 850 to 1200°C.(2-4) The mechanism for this acceleration is geometrically identical to that proposed for the solution-precipitation step of liquid phase sintering (5) and for solid state sintering by a grain boundary diffusion mechanism. (6) As a result, the present authors have proposed that carrier phase sintering using either a liquid phase or a solid "activating" element is the selective acceleration of mass transport by interfacial diffusion.(4)

In the present investigation, the densification of

pure tungsten in the pre-sintering temperature range was studied. The results indicate that sintering arises from grain boundary diffusion, and establish two points: the pre-sintering of tungsten is an example of the proposed but hitherto unobserved grain boundary mass transport path in sintering, and "carrier phase sintering" selectively modifies the interfacial diffusion mechanism. It was also observed that small amounts of iridium added to tungsten decelerate, rather than accelerate interfacial diffusion transport.

EXPERIMENTAL PROCEDURE

Compacts of commercially pure tungsten were pressed at 26,000 psi from Wah-Chang C-5 tungsten powder having a BET particle size of 0.56 microns. The linear dimensions of the compacts were measured; the average pressed dimensions being 2 in. by 1/8 in. square. The pressed samples were inserted rapidly into wire wound furnaces at temperatures ranging from 1050 to 1200°C under purified hydrogen. After sintering the samples were again measured and linear shrinkage was calculated. Most of the sintering results were gathered by making successive heat treatments on an individual compact. Equivalent results were obtained using either individual samples for each sintering time,

or accumulating times on a single sample.

Iridium-tungsten powders were prepared by dissolving the desired amount of iridium as iridium chloride in water and adding this to C-5 tungsten powder. The water was evaporated overnight in a drying oven at 150°C. The resulting powder cake was ground in a mortar and pestle and the powder was reduced in hydrogen at 800°C for one hour. Samples were pressed and sintered in a manner identical to that of the pure tungsten compacts.

RESULTS AND DISCUSSION

The results of linear shrinkage as a function of sintering time for pure Wah-Chang C-5 tungsten powder at temperatures ranging from 1050 to 1200°C are shown in Figure 1. Linear shrinkage increases with the cube root of time at all temperatures. This is the time dependence which Coble (6) predicted for the two sphere sintering model when grain boundary diffusion is the rate controlling step leading to densification. Because of the low volume self diffusivity of tungsten at these temperatures and the inability of a surface diffusion process to lead to overall densification (7), it is

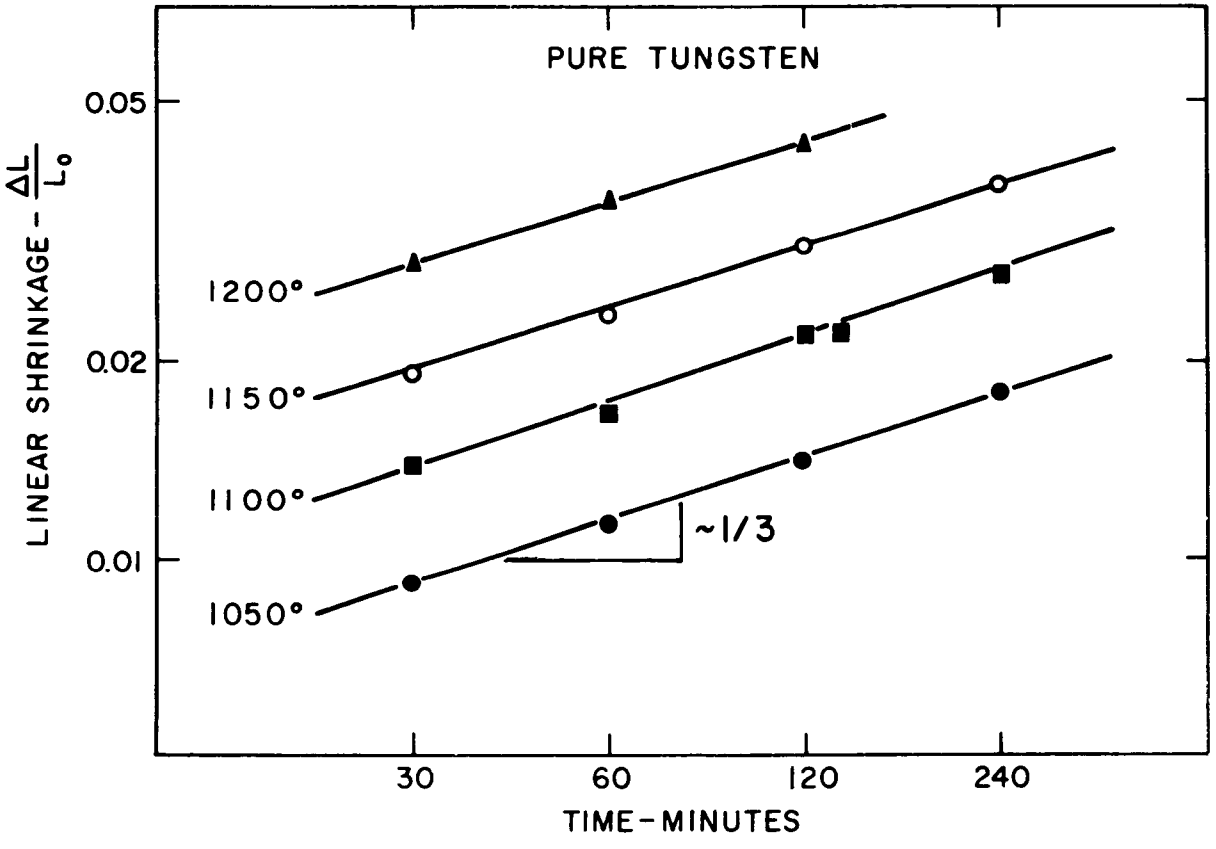

Figure 1: Time Dependence of Linear Shrinkage for Pure C-5 Tungsten Compacts.

indeed reasonable that grain boundary diffusion would be rate controlling for densification at these temperatures. On the basis of the data in Figure 1, an activation energy of 90,000 cal/mol has been calculated by plotting the time necessary to attain 5% linear shrinkage (by extrapolation of the experimental data) versus the reciprocal of the absolute sintering temperature. Although the activation energy for tungsten grain boundary self-diffusion has not been previously determined by other techniques, the results of the present investigation are in precise agreement with that which Langmuir obtained for the grain boundary diffusion of thorium in tungsten.(8)

The extent of linear shrinkage in tungsten at these temperatures, as indicated in Figure 1, is very small, but definitely measureable. Since the temperatures involved in this investigation are in the conventional pre-sintering range for tungsten, the strengthening effect of pre-sintering appears to be due to a small amount of densification and interparticle bonding resulting from the grain boundary diffusion process.

When tungsten is sintered at temperatures between 1050 and 1200^{o}C in the presence of small amounts of iridium,

the rate of densification is less than that of pure tungsten. This deceleration is contrary to the acceleration of densification in tungsten sintered with comparable amounts of other Group VIII transition elements. (4) The effect of iridium content is shown in Figure 2. After a given sintering treatment, linear shrinkage decreases with increasing iridium content up to 1.5 weight percent, after which it is independent of further increases in iridium content. Figure 3 shows the time dependence of linear shrinkage for compacts containing 4 weight percent iridium. At all temperatures shrinkage increased with the 0.38 power of time. This power lies between the theoretically predicted value of 0.33 if diffusion of tungsten atoms in a tungsten-iridium interface were rate controlling, and the value of 0.40 if volume diffusion of tungsten were rate controlling. (7) The activation energy of 133,000 cal/mol shown in Figure 4 calculated from the data in Figure 3 is close to the value of 135,000 cal/mol for the volume self diffusion of tungsten. (9) On the basis of the experimental findings it is difficult to establish whether tungsten interfacial diffusion or volume diffusion is the rate controlling step leading

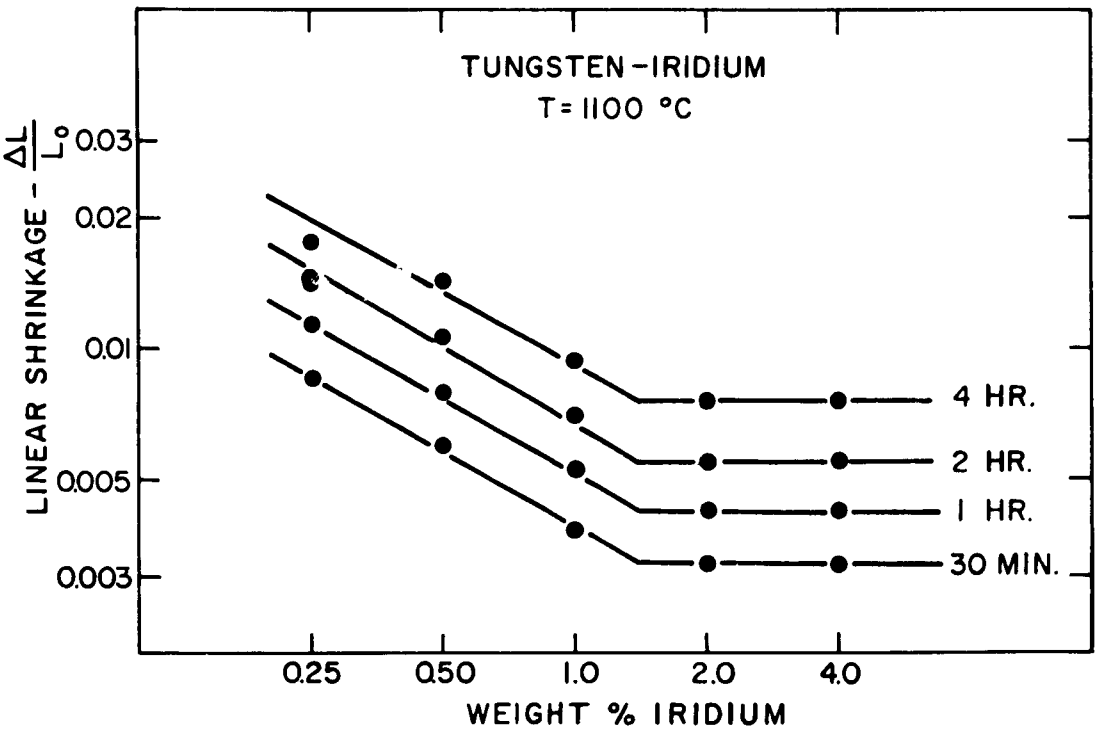

Figure 2: Composition Dependence of Linear Shrinkage for Iridium-Tungsten Compacts.

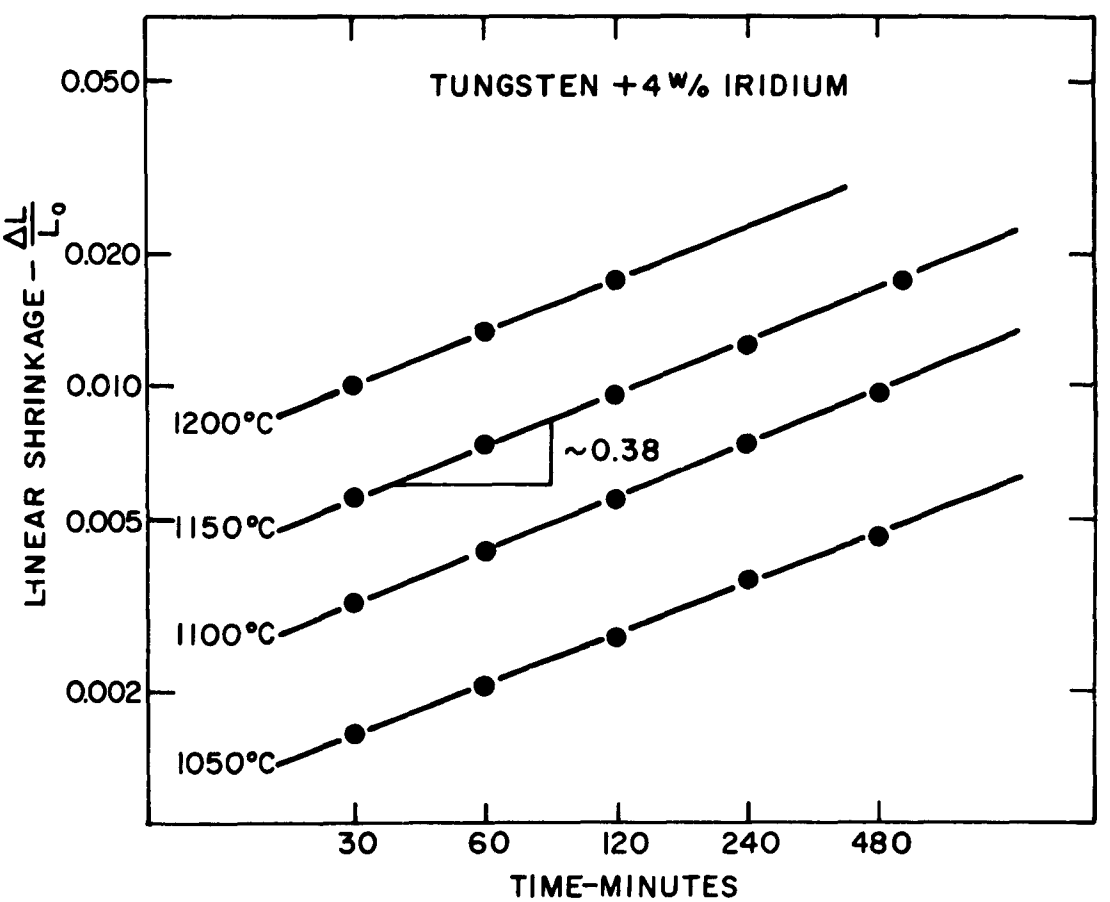

Figure 3: Time Dependence of Linear Shrinkage for Iridium-Tungsten Compacts.

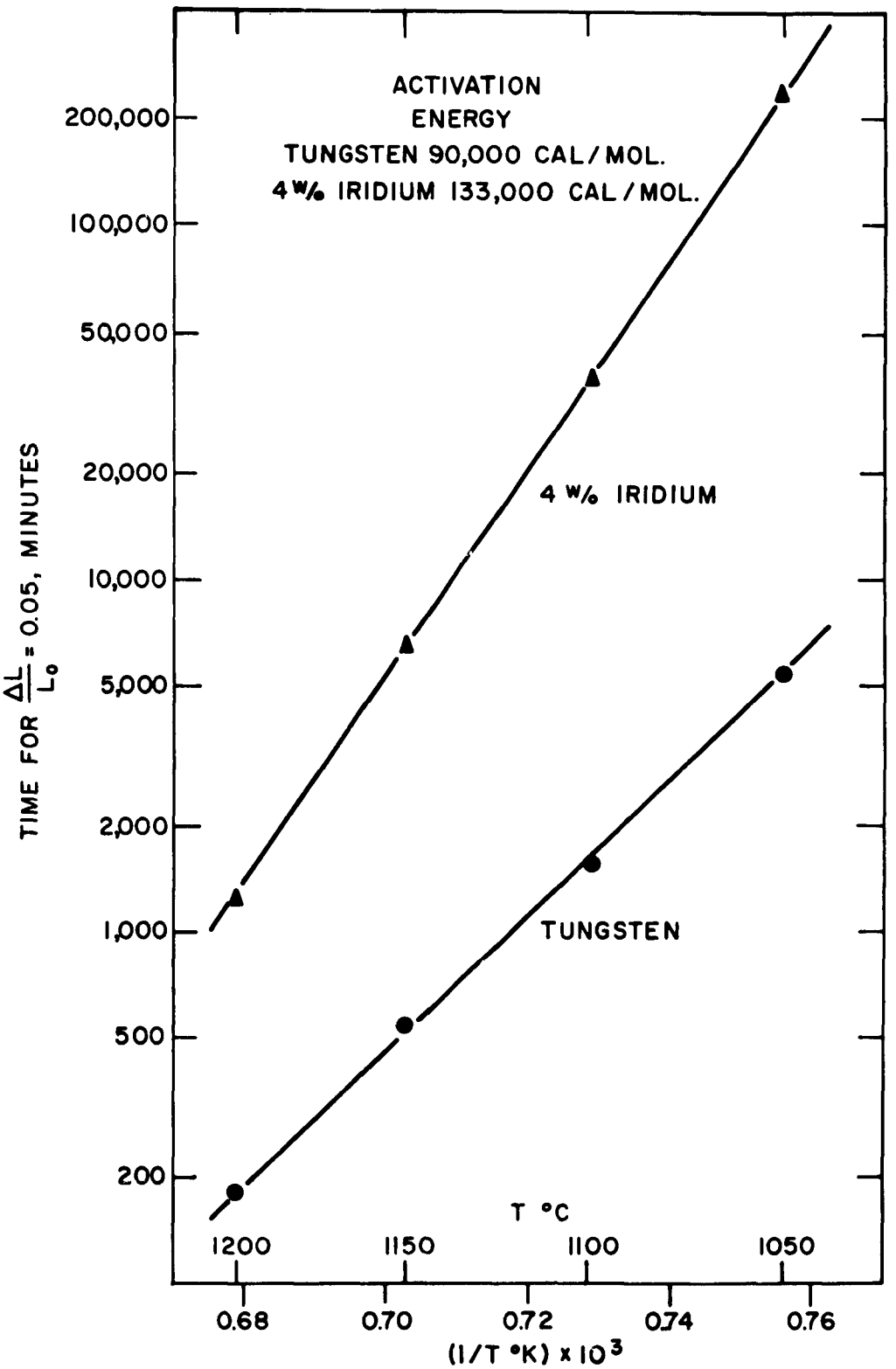

Figure 4: 'Arrhenius' Plots from Data from Sintering of Pure Tungsten and Iridium Tungsten.

to densification in this case. However, it is definitely established that the formation of a continuous layer of iridium on the surfaces of tungsten particles retards the rate of tungsten interfacial transport. This observation is a corrolary to the recent finding that a plated iridium layer gives oxidation protection to tungsten articles (10), presumably by serving as a barrier through which the diffusion of tungsten is extremely slow.

The experimental results in the sintering of pure tungsten are the first direct observation in which grain boundary diffusion is the controlling step leading to densification. The addition of iridium to tungsten decelerates the characteristic inter-facial diffusion process, possibly to the extent that the volume self-diffusion of tungsten becomes significant. These results, generally, substantiate the previous interpretation that the rapid sintering of tungsten powders containing certain other Group VIII transition metals results from a modification of the rate of inter-facial diffusion of tungsten atoms.

CONCLUSIONS

The small amounts of densification observed in the pre-sintering of tungsten result from the grain boundary diffusion of tungsten atoms. The activation energy of this process is 90,000 cal/mol. This mechanism can account for the strengthening commonly observed after pre-sintering at 1000 to 1200°C.

Additions of iridium to tungsten powder decelerate the interfacial diffusion of tungsten atoms possibly to the extent that volume self-diffusion of tungsten atoms becomes a significant step leading to the small degree of densification. The activation energy for this process is 133,000 cal/mol.

The present results strengthen the previous interpretations of "activated" sintering of tungsten with small additions of certain Group VIII transition metals. Iridium causes a deceleration, while the others cause an acceleration of the characteristic interfacial transport of tungsten atoms.

BIBLIOGRAPHY

1. J. Vacek, "On Influencing the Sintering of Tungsten", Planseeberichte fur Pulvermetallurgie, 7 (1959) p. 6.

2. J.H. Brophy, L.A. Shepard, J. Wulff, "Nickel Activated Sintering of Tungsten", Powder Metallurgy, ed. by W. Leszynski, AIME, MPI Interscience, New York (1961) p. 113.

3. J.H. Brophy, H.W. Hayden, J. Wulff, "Final Stages of Densification of Nickel Tungsten Compacts", Trans. AIME, 224 (Aug., 1962) p. 797.

4. H.W. Hayden, J.H. Brophy, "The Activated Sintering of Tungsten with Group VIII Elements", Submitted for publication.

5. W.D. Kingery, "Densification During Sintering in Presence of a Liquid Phase, I. Theory," J. App. Phys, 30 (1959) No. 3, p. 301.

6. R.L. Coble, "Diffusion Sintering in the Solid State", Kinetics of High Temperature Processes, ed. by W.D. Kingery, Tech. Press-Wiley (1959) p. 147.

7. W.D. Kingery, M. Berg, "Study of Initial Stages of Sintering Solids by Viscous Flow, Evaporation-Condensation, and Self Diffusion," J. App. Phys., 26 (1955) p. 1205.

8. I. Langmuir, "Thoriated Tungsten Filaments," J. Franklin Inst., 217 (1934) p. 543.

9. C.J. Smithells, Metals Reference Book, Vol. II, Butterworths, Washington (1962) p. 598.

10. E.M. Passmore, J.E. Boyd, L.P. Neal, C.A. Andersson, B.S. Lement, "Investigation of Diffusion Barriers for Refractory Metals," WADD Technical Report 60-343 (Aug., 1960).

PART III

THE ROLE OF PHASE RELATIONSHIPS IN THE ACTIVATED SINTERING OF TUNGSTEN

INTRODUCTION

The effects of certain Group VIII transition metals on the sintering rates of tungsten at temperatures below those at which a liquid phase would be predicted have recently been investigated by the present authors[1-4]. It was found that small additions of palladium, nickel, rhodium, platinum, and ruthenium accelerate the rate of tungsten sintering. Additions of iridium decelerated the rate of densification compared to that of pure tungsten in the same temperature range. In all cases the rate of densification changed with increasing amounts of these additions, up to those compositions at which a continuous layer was formed on the surfaces of the tungsten powder particles. The rate of densification was then independent of further increases of the compositions of any of these addition elements.

On the basis of the observed densification behavior, it was concluded that each of these additions

formed interfaces with tungsten in which tungsten diffusivity was either greater or less than its grain boundary self-diffusivity. In all of these cases, with the singular exception of nickel at temperatures below approximately 950°C, the equilibrium diagrams predict extensive composition width solid solutions or intermediate phases in equilibrium with essentially pure tungsten.[5-8] Iron, cobalt, and nickel at temperatures below 950°C, are known to accelerate densification, but their equilibrium diagrams predict narrow composition width intermetallic compounds.[5] The present investigation was conducted in attempt to find the effect of intermetallic compound formation on the sintering kinetics of tungsten powders with small additions of iron and cobalt.

EXPERIMENTAL PROCEDURE

The tungsten powder employed in this investigation was hydrogen-reduced powder of 0.56 micron BET average particle diameter purchased from the Wah-Chang Corporation. Cobalt and Iron were obtained in the form of reagent grade nitrates.

The "activator" compounds were weighed to yield

the desired amount of the element, were dissolved in water and mixed with the necessary amount of tungsten powder. After overnight evaporation in air at 150°C, the resulting powder cake was broken manually and reduced in hydrogen at 800°C for one hour. Specimens approximately 2 inches by 1/8 inch square were pressed in an unlubricated steel die at 26,000 psi. Each specimen was then measured in linear dimensions.

Sintering was accomplished by rapidly inserting an alundum boat containing the sample into a wire-wound furnace pre-heated to the desired temperature. At all times the sample was held under purified hydrogen when above room temperature.

After sintering, linear dimensions were again recorded. The sample was again inserted into the furnace and by duplicating the above procedure, accumulated sintering times were gained on a single sample.

RESULTS AND DISCUSSION

The results of this investigation are presented in Figures 1 through 4. These show both the time and addition element composition dependences of linear

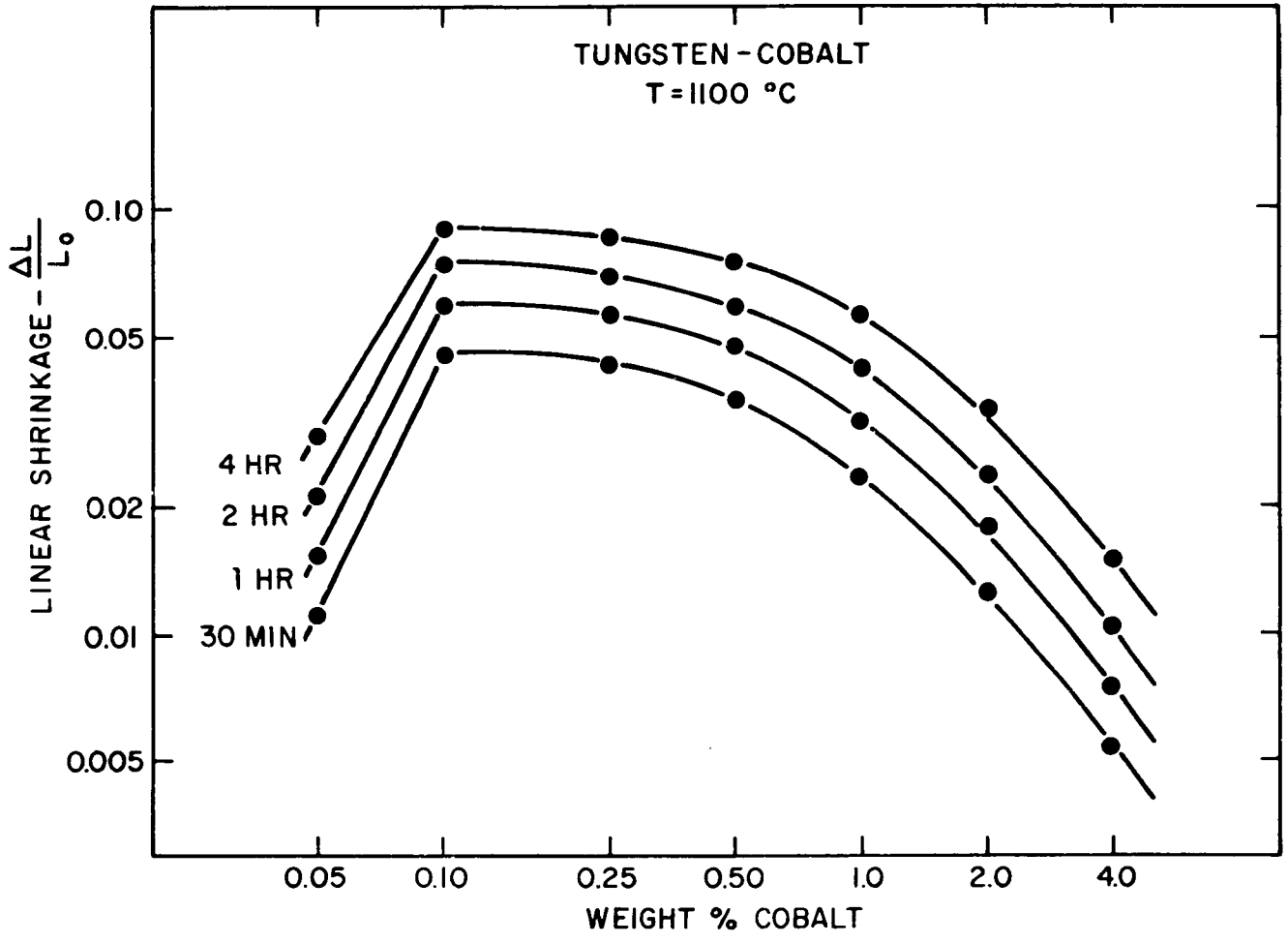

Figure 1: Composition Dependence of Linear Shrinkage for Cobalt-Tungsten Compacts.

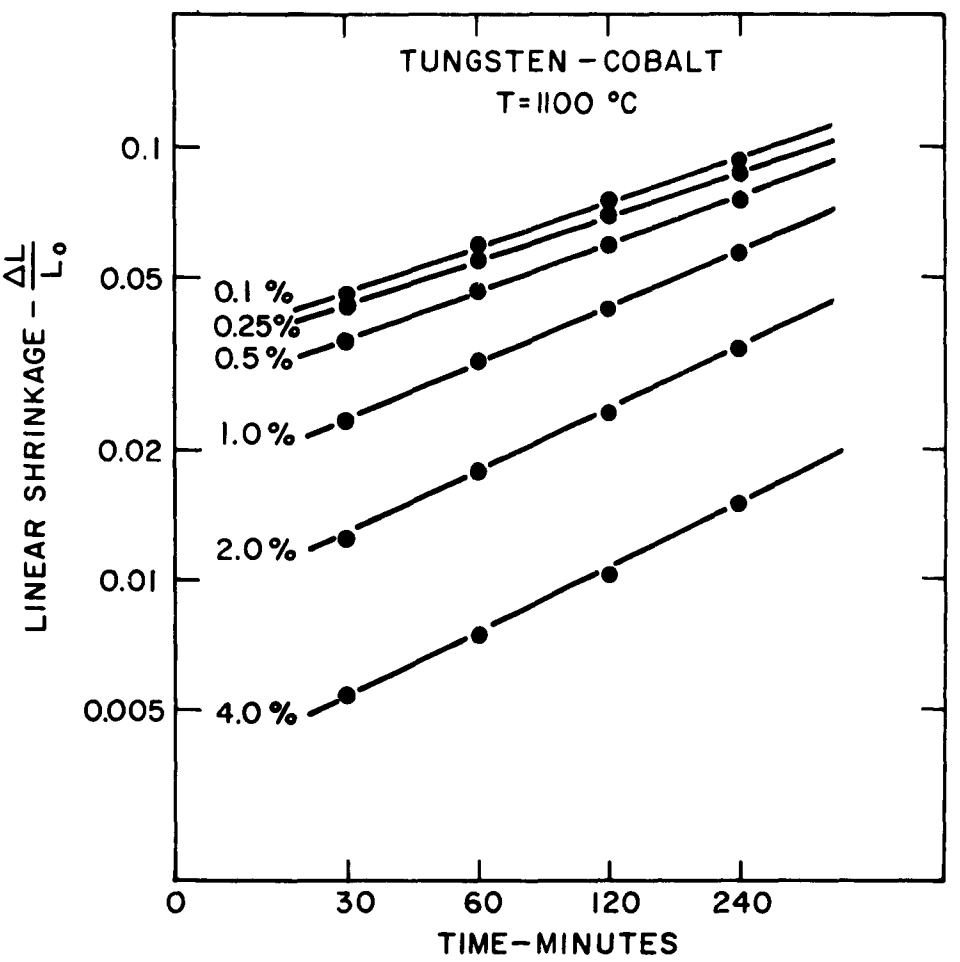

Figure 2: Time Dependence of Linear Shrinkage for Cobalt-Tungsten Compacts.

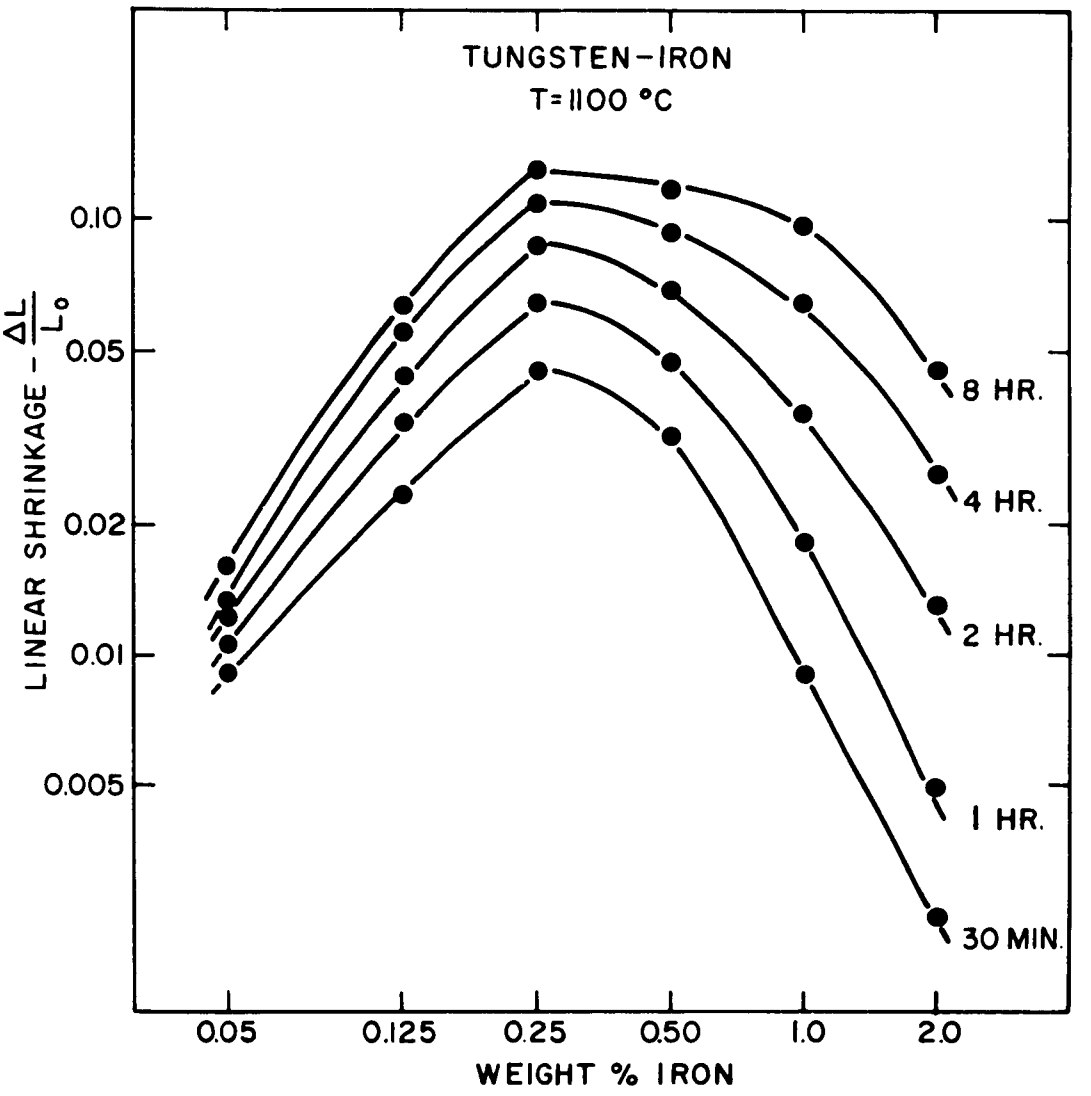

Figure 3: Composition Dependence of Linear Shrinkage for Iron-Tungsten Compacts.

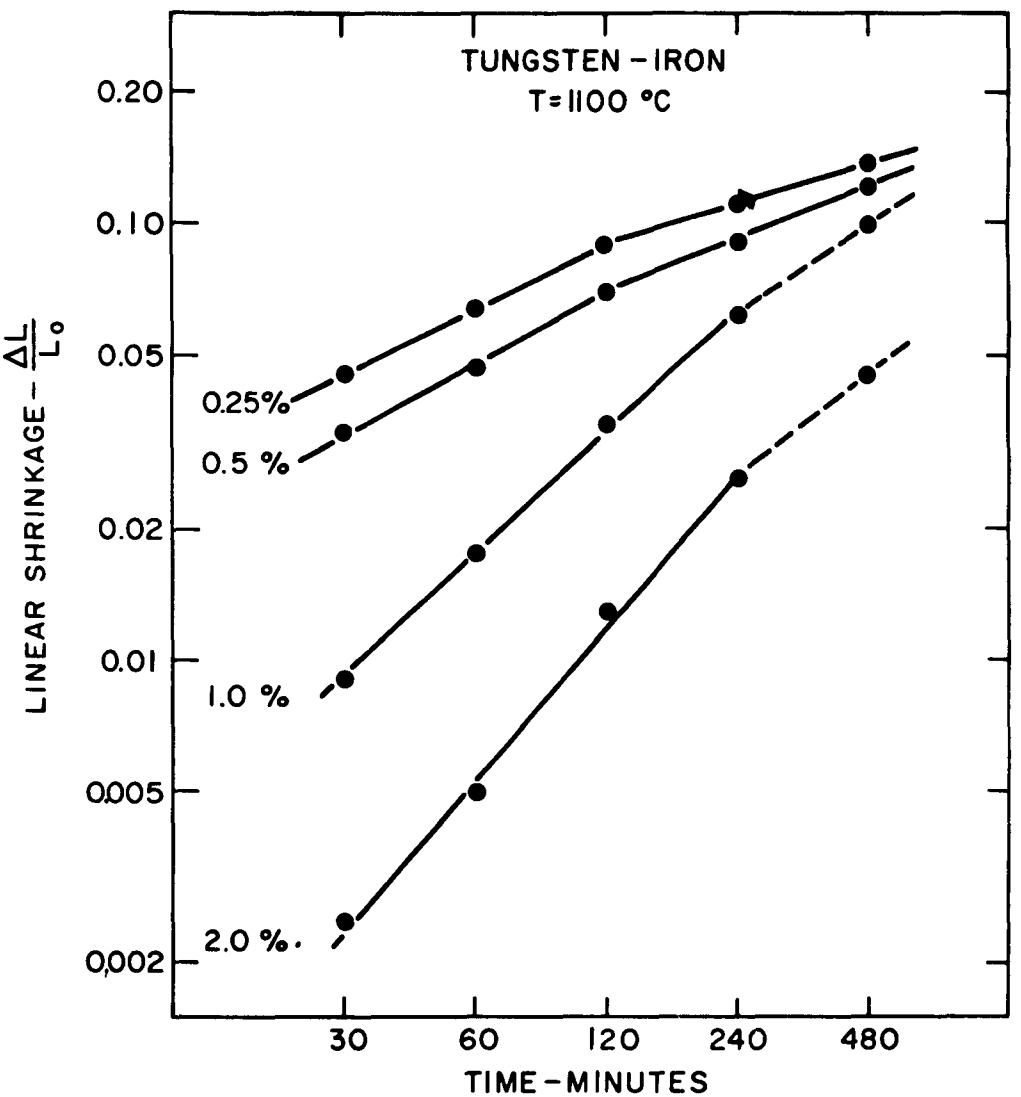

Figure 4: Time Dependence of Linear Shrinkage for Iron-Tungsten Compacts.

shrinkage for compacts of tungsten containing small additions of cobalt or iron sintered at 1100°C. The phase diagrams predict that essentially pure tungsten should be in equilibrium with the intermetallic compounds W_6Co_7 or W_2Fe_3.[5]

In all cases, both the degree and time dependence of linear shrinkage are highly dependent on the composition of the addition element. For a given sintering condition, linear shrinkage increases with increasing composition up to 0.1 weight percent cobalt (Figure 1) and 0.25 weight percent iron (Figure 3). These particular compositions would correspond to amounts necessary to form slightly less than a monolayer of cobalt and a dilayer of iron on the surfaces of the particular size tungsten particles employed. After the maximum shrinkage is attained at these compositions, shrinkage then decreases with further increases in composition. In all the Group VIII-tungsten systems previously studied, no such decrease was observed.[1-4]

In the case of tungsten containing 0.1 weight percent cobalt, linear shrinkage increases with the cube root of time (Figure 2). In the case of 0.25 weight percent iron (Figure 4) linear shrinkage varies

with the square root of time. From previous analyses[1,3] this would suggest diffusion and solution control, respectively, via an interfacial transport path. However in each system, larger amounts of the added elements reduced the amount of shrinkage and increased the power of the time dependence of the shrinkage process.

It is interesting to compare the results obtained in this investigation with nickel-tungsten results reported previously[1]. When sintering was conducted at temperatures above the peritectoid decomposition point of WNi_4, linear shrinkage was independent of increases in nickel content above that necessary to form a monolayer of nickel on the tungsten particle surfaces. Similar independence of addition element composition has been observed in the sintering of tungsten with additions of the platinum metals (except osmium which has not been investigated).[3,4] In all cases where independence of addition element composition was observed, the phase diagrams predict that tungsten should be in equilibrium with solid solutions or intermediate phases of extensive composition width.[5-8] In this investigation, X-Ray diffraction revealed that with

2 weight percent iron and four weight percent of each other Group VIII elements, the phase predicted to be in equilibrium with tungsten was present in crushed sintered alloys. In the cases of Fe and Co these were the respective intermetallic compounds. In the cases of Pt, Pd, Ru, and Ni above 950°C, these were terminal solid solutions rich in the Group VIII element. In the cases of Ir and Rh, these were HCP intermediate phases.

These results suggest a tentative explanation for the influence of nickel at low temperatures[1], cobalt and iron on tungsten sintering. As the amounts of the added elements increase to the point where a continuous layer is formed, the rate of sintering increases. With these very small amounts the layers are probably epitaxial with the tungsten surfaces. However, with increasing amounts of the added element, there is a continuous trend from an epitaxial layer of atoms to the formation of a layer having the equilibrium structure of the bulk intermetallic compound. Since the stable composition range of these compounds indicates high binding energy, it is likely that tungsten diffusivity through them is low. Apparently as the compound layer

assumes its true bulk properties, it retards tungsten diffusivity through its interface with tungsten and therefore retards densification.

CONCLUSIONS

Additions of those Group VIII transition metals to tungsten powders which form intermetallic compounds produce a different sintering behavior than is observed in the cases of those additions which form extensive composition width solid solutions or intermediate phases. Linear shrinkage of powder compacts containing additions of iron or cobalt increases with increasing iron or cobalt composition to that point at which a continuous layer of either of these additions is formed on the surfaces of the tungsten powders. With further increases in the composition of either of these additions linear shrinkage decreases, while in all other Group VIII-tungsten systems, shrinkage is independent of the Group VIII metal composition beyond those compositions necessary to form continuous layers. This effect has been tentatively explained by the continuous trend from the existence of an epitaxial layer of either

iron or cobalt at low composition levels to the formation of layers having the properties of the respective intermetallic compounds at higher compositions. Due to the narrow composition width of these compounds, high bonding energies and thus low diffusivities would be expected.

BIBLIOGRAPHY

1. J.H. Brophy, L.A. Shepard, J. Wulff, "Nickel Activated Sintering of Tungsten," Powder Metallurgy, ed. by W. Lyszynski, AIME, MPI, Interscience, New York, 1961, p. 113.

2. J.H. Brophy, H.W. Hayden, J. Wulff, "Final Stages of Densification of Nickel Tungsten Compacts," Trans. AIME, 224, August, 1962. p. 797.

3. H.W. Hayden, J.H. Brophy, "The Activated Sintering of Tungsten with Group VIII Transition Metals," to be published by the Journal of the Electrochemical Society.

4. H.W. Hayden, J.H. Brophy, "Grain Boundary Diffusion in Tungsten Sintering," submitted for publication.

5. M. Hanson, Constitution of Binary Alloys, McGraw-Hill, New York, 1958, pp. 518, 732, 1058, and 1145.

6. M.A. Tylkina, V.P. Polykova, Ye.M. Savitskiy, "Constitution Diagram of the Palladium Tungsten System," Zhurnal Neorganicheskoy Khimii, 6, 1961, No. 6, p. 1471.

7. E.J. Rapperport, M.F. Smith, Refractory Metal Constitution Diagrams, Tech. Doc. Rep. No. WADD TR 60-132 Part II, Sept., 1962, pp. 17 & 27.

8. E.J. Rapperport, M.F. Smith, Refractory Metal Constitution Diagrams, WADD Tech. Rep. 60-132 (NMI-9216), June, 1960, p. 26.

PART IV

THE RELATIONSHIP BETWEEN LIQUID PHASE SINTERING AND ACTIVATED SINTERING OF TUNGSTEN

INTRODUCTION

The low temperature densification of tungsten can be accelerated by the presence of small amounts of a number of other elements, either in the liquid or in the solid state. Nickel[1] and copper-nickel[2] liquids and solid iron, cobalt, or nickel[3] have been added to tungsten by previous investigators. More recently a kinetic analysis of the influence of nickel on tungsten densification has been completed[4,5], and it was found that most of the Group VIII transition elements modified tungsten sintering[6]. The path and kinetics of mass transport have been found to resemble those proposed by Kingery for liquid phase sintering[7] and by Coble for a postulated grain boundary mechanism in solid state sintering[8].

As a result it has been proposed that solid state activated sintering and liquid phase sintering together comprise a general type of carrier phase sintering which selectively modifies an available mass transport path[6]. In the case of tungsten this available path

is the interparticle boundary found to govern sintering of pure tungsten at 1100°C[9]. When a carrier phase is present, mass transport is accelerated in the carrier phase-tungsten interface.

It is the purpose of this investigation to examine the postulate that activated sintering and liquid phase sintering are two special cases of carrier phase sintering, and to determine the influence of copper dissolved in the nickel during the activated sintering of tungsten.[6] Tungsten-copper-nickel alloys were sintered in the presence of either a solid or a liquid phase. An attempt was made to eliminate the effect of rearrangement[7] in the liquid to show the similarity between the solution-precipitation stages in both solid and liquid carrier phase sintering. In this type of process the solubility of tungsten in the carrier phase appears in the calculated constant of proportionality between linear shrinkage and time.[4] Therefore, as the nickel carrier phase is diluted with copper, linear shrinkage at constant time, temperature, and tungsten particle size should decrease due to the decrease in solubility of tungsten. In studying these effects a range of matrix alloy compositions and the influence of diffusional porosity were investigated.

EXPERIMENTAL PROCEDURE

All tungsten powder was hydrogen reduced. Wah Chang Corp. C-5, C-10 and C-20 powders were used at various times. The microscopic average particle sizes for these powders are 1.11, 2.66 and 4.07 microns respectively.

Tungsten-copper-nickel alloys containing 97-99.9 w/o tungsten were prepared by the co-reduction of $Ni(NO_3)_2$ and $Cu(NO_3)_2$ hydrated salts. The tungsten powder was stirred into an aqueous solution of the copper and nickel salts. The water was evaporated in a drying oven. Reduction and matrix alloy homogenization were carried out at 800°C for 24 hours under a hydrogen atmosphere.

In the preparation of high matrix content alloys, co-reduction was impossible because of the exothermic decomposition of copper salts, so copper and nickel were added as elemental powders. Mixing was achieved by wire milling on a lathe. Milling times were of the order of 12 hours.

Compacts were pressed in an unlubricated steel die at a pressure of 31,000 psi. Green lengths

ranged from 2.0000-2.0100 inches. Width was 0.180 inches and green thicknesses ranged from 0.170-0.190 inches. Green densities ranged from 50-54% of theoretical density for the C-5 powder, while C-10 and C-20 powders yielded green densities of 60% and 65% of theoretical density respectively.

All sintering was performed under a hydrogen atmosphere. One minute was allowed for both specimen heat-up and cool-off. Specimen length was measured at various times during the sintering process using a micrometer. All bars were sintered in alundum boats. Specimens were quenched by pulling the boat out of the hot zone, leaving it in protective atmosphere. Upon sufficient cooling to prevent oxidation the specimens were removed from the atmosphere and measured. It was found that shrinkages measured for small time increments were arithmetically additive. Therefore, a series of shrinkages versus time could be obtained using one bar. Spot checks of reproducibility, using new bars, were made.

Temperatures up to 1100^{o}C were obtained using chromel wound vycor furnaces. Silicon carbide (Globar)

heating element furnaces were employed from 1100-1500°C, using mullite muffles. In order to remove specimens from the Globar hot zone without thermally shocking the ceramic combustion tube a ½ inch thick molybdenum bar was inserted to act as a runner between the cool and hot zones.

Iron-copper alloys were prepared by wire milling -325 mesh copper powder and either carbonyl or Swedish sponge iron powder. To improve the pressability of the copper plus carbonyl iron mixtures, CCl_4 was added as a binder. It was vaporized before subsequent sintering. The compacting pressure was reduced to 28,000 psi.

Compacts of copper plus nickel for Kirkendall porosity studies were prepared by wire milling and pressing. Pressing pressures were 28,000-31,000 psi. Various binary combinations of -150 and -325 mesh copper powder and -150 and -325 mesh nickel powder were prepared. Expansion was measured as negative linear shrinkage.

EXPERIMENTAL RESULTS AND DISCUSSION

In the activated sintering of tungsten, it has been proposed that decreased solubility of tungsten in the activating matrix should result in decreased shrinkage rate, and that activated sintering and liquid phase sintering are two special cases of a general process called carrier phase sintering.[4] The primary purpose of this investigation was to examine the validity of these two proposals. The results may be divided into four general categories: 1) the influence of tungsten solubility on sintering with the nickel activator phase diluted with copper, 2) the liquid phase sintering of tungsten in the same copper-nickel alloys, 3) the transition from solid to liquid phase sintering, and 4) a corollary study of diffusional (Kirkendall) porosity encountered in solid phase sintering of copper-nickel-tungsten. In this study copper was employed as a diluent for nickel because it can be expected to reduce the solubility of tungsten and to lower the matrix alloy melting point, and also because the resultant product resembles the familiar

heavy alloys.[2]

1) The Influence of Solubility in Solid Carrier Phase Sintering

Alloys of C-5 tungsten powder (1.11 micron average particle size) with small additions of copper-nickel-matrix alloy were sintered in the temperature range 900-1100°C. Powders were prepared by co-reduction and pre-diffusion to prevent formation of Kirkendall porosity in the matrix. Matrix alloy compositions investigated were 3Ni:1Cu, 1Ni:1Cu, and 1Ni:3Cu. Table I is a compilation of 99 w/o tungsten solid phase sintering data. Figure 1 is a representative solid phase sintered microstructure, showing sharp corners on tungsten particles.

Figures 2-4 show linear shrinkage as a function of time and temperature for the three matrix compositions in 99 w/o tungsten alloys. The change in slope apparent during sintering is indicative of a change in rate controlling process. Both solution of tungsten into the carrier phase and diffusion of tungsten outward from the line of particle centers occur during the solution-precipitation process.

TABLE I

SHRINKAGE DATA FOR 99 w/o TUNGSTEN ALLOYS SINTERED IN THE SOLID PHASE

3Ni:1Cu

	time (min.)	length (in.)	$\Delta L/L_o$
900°C	0	2.0050	
	30	1.9570	0.015
	60	1.9627	.021
	120	1.9423	.031
	240	1.9228	.041
	480	1.8925	.056
	720	1.9736	.066
950°C	0	2.0057	
	30	1.9411	.032
	60	1.9154	.045
	120	1.8822	.062
	240	1.8446	.080
	480	1.8012	.102
	720	1.7713	.117
1000°C	0	2.0052	
	30	1.8894	.059
	60	1.9527	.076
	120	1.8095	.098
	240	1.7640	.120
	360	1.7361	.134
	480	1.7193	.143
1050°C	0	2.0049	
	30	1.8316	.086
	60	1.7787	.108
	120	1.7415	.132
	240	1.6976	.153
	360	1.6760	.164
	480	1.6624	.171

	time (min.)	length (in.)	$\Delta L/L_o$
1050°C	0	2.0049	
	30	1.8316	.086
	60	1.7787	.108
	120	1.7415	.132
	240	1.6976	.153
	360	1.6760	.164
	480	1.6624	.171
1100°C	0	2.0071	
	30	1.7530	.127
	60	1.7196	.143
	120	1.6841	.161
	180	1.6645	.171
	240	1.6509	.177
1Ni:1Cu			
900°C	0	2.0048	
	30	1.9792	.013
	60	1.9672	.019
	120	1.9468	0.029
	240	1.9260	.039
	480	1.8987	.053
	640	1.8811	.062
950°C	0	2.0042	
	30	1.9439	.030
	60	1.9208	.042
	120	1.8941	.055
	240	1.9588	.073
	480	1.8150	.094
	675	1.7121	.106
1000°C	0	2.0044	
	30	1.8970	.054
	60	1.9655	.069
	120	1.8221	.091
	240	1.7750	.114
	360	1.7491	.127
	480	1.7315	.136
	720	1.7065	.149

	time (min.)	length (in.)	$\Delta L/L_o$
1050°C	0	2.0048	
	30	1.8480	.078
	60	1.8037	.100
	120	1.7540	.125
	240	1.7090	.148
	360	1.6876	.158
	480	1.6722	.166
1100°C	0	2.0062	
	30	1.7726	.118
	60	1.7355	.136
	120	1.6999	.154
	180	1.6819	.163
	240	1.6683	.170
1Ni:3Cu			
900°C	0	2.0035	
	30	1.9886	.0074
	60	1.9827	.010
	120	1.9744	.015
	240	1.9601	.022
	480	1.9408	.031
	720	1.9284	.038
950°C	0	2.0038	
	30	1.9805	.012
	60	1.9683	.018
	120	1.9557	0.024
	240	1.9357	.034
	480	1.9071	.048
	720	1.8864	.059
1000°C	0	2.0042	
	30	1.9576	.023
	60	1.9414	.031
	120	1.9177	.043
	240	1.8853	.059
	360	1.8587	.073
	480	1.8385	.083

	time (min.)	length (in.)	$\Delta L/L_o$
1050°C	0	2.0042	
	30	1.9316	.036
	60	1.9023	.051
	120	1.8645	.070
	240	1.8249	.089
	360	1.7964	.104
	480	1.7742	.115
1100°C	0	2.0038	
	30	1.8888	.057
	60	1.8463	.079
	120	1.8014	.101
	240	1.7509	.126
	360	1.7200	.142

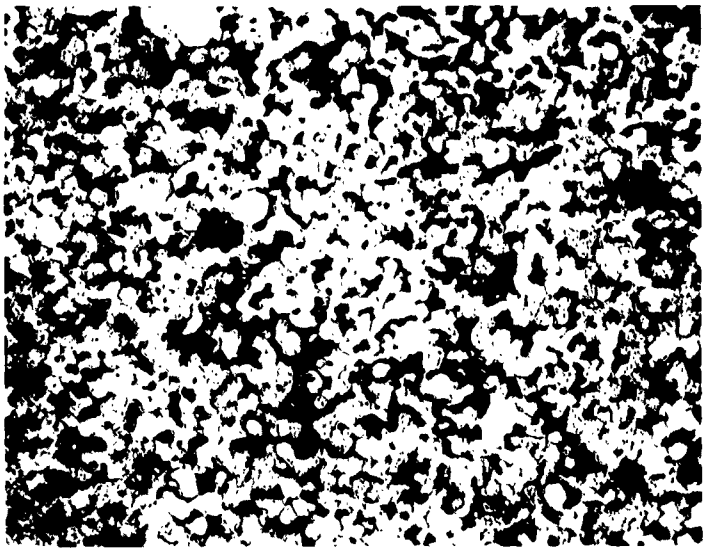

Figure 1: Sample of 99W-0.75Ni-0.25Cu Sintered at 1100°C for 4 Hourse Etched with Wolff's Reagent. 500X

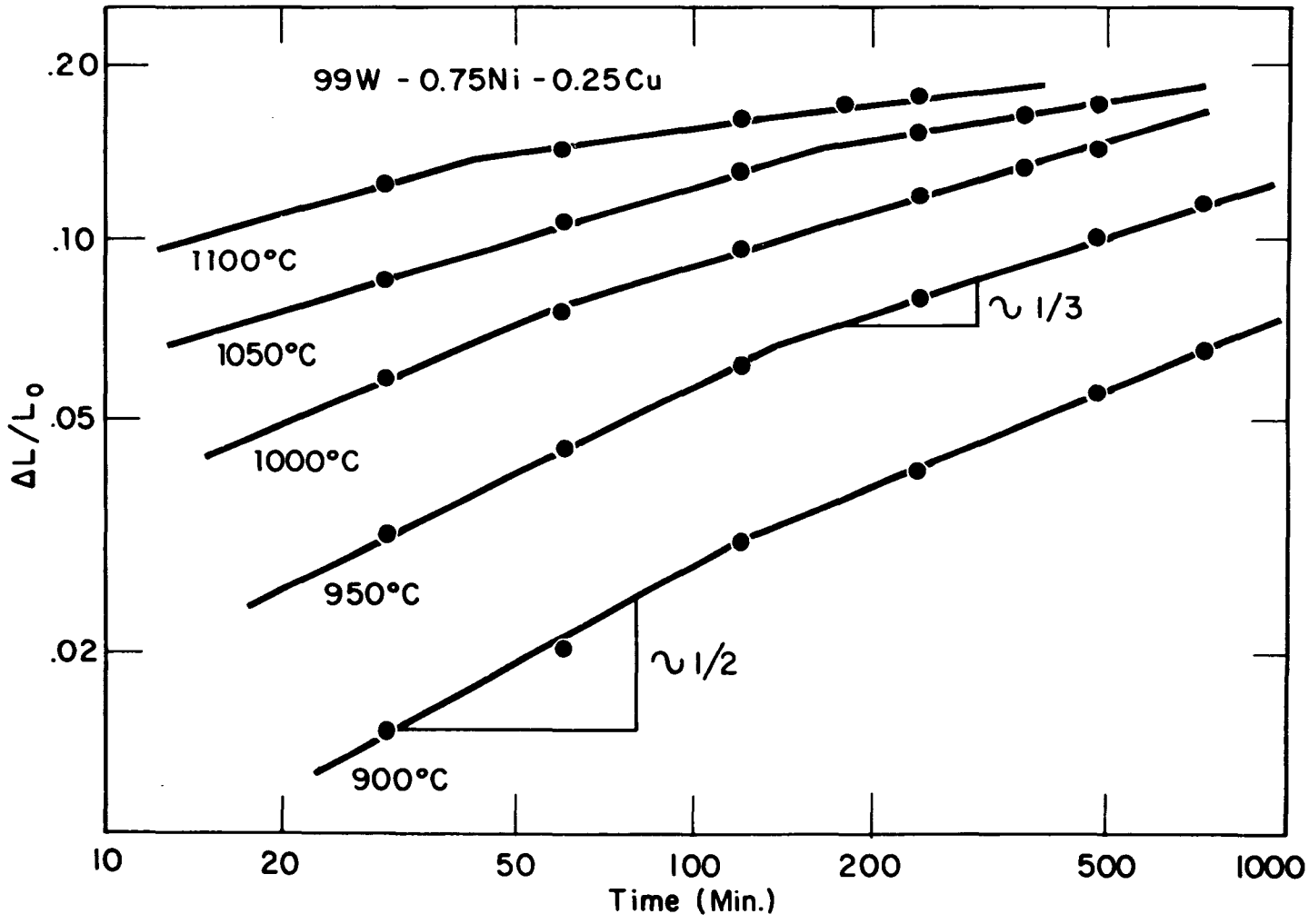

Figure 2: Linear Shrinkage as a Function of Time and Temperature for 99W-0.75Ni-0.25Cu Alloys.

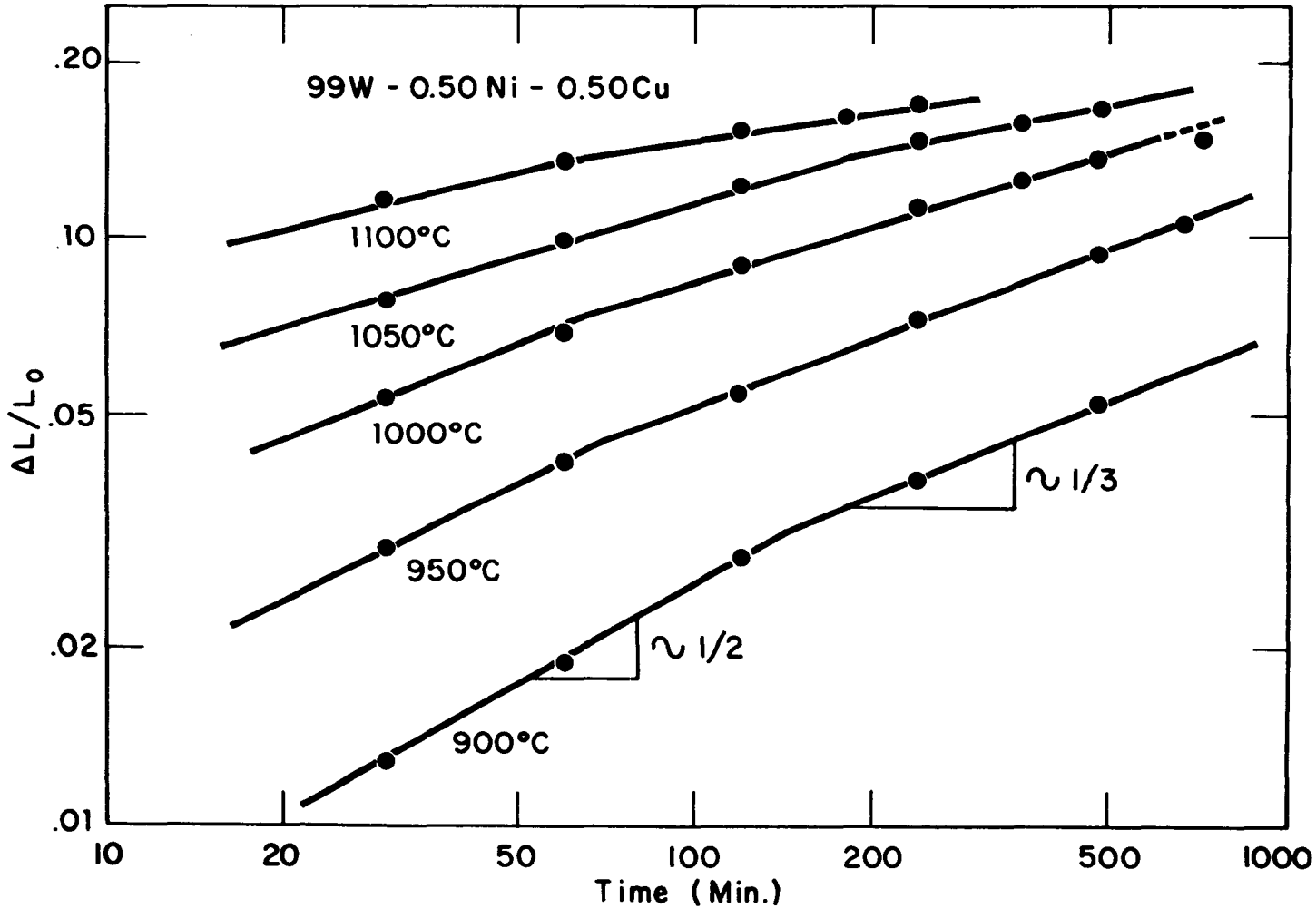

Figure 3: Linear Shrinkage as a Function of Time and Temperature for 99W-0.50Ni-0.50Cu Alloys.

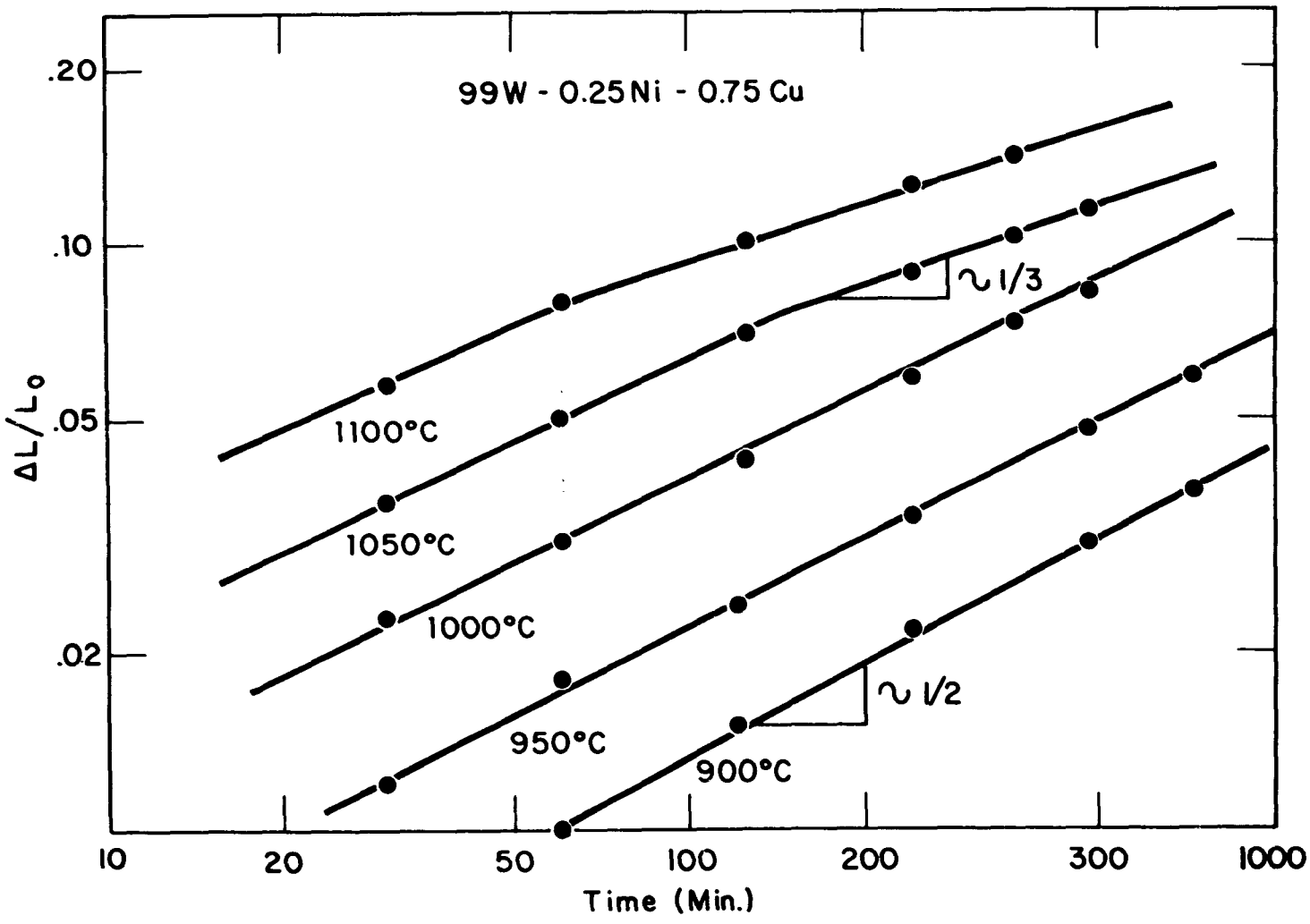

Figure 4: Linear Shrinkage as a Function of Time and Temperature for 99W-0.25Ni-0.75Cu Alloys.

Since the two are sequential in nature, that process is rate controlling which produces the slower linear shrinkage rate. Early in the sintering process the interparticle flat area, in which solution occurs, is very small. Therefore, tungsten solution is rate controlling. With increased shrinkage the area for solution rises, but the diffusional flux remains constant. Therefore, at some intermediate shrinkage, diffusion becomes rate controlling. This is indicated in Figures 2-4, beginning with slopes of ½ and shifting to slopes of 1/3 at some intermediate value of shrinkage. Shrinkage values at which the change occurs vary with temperature, due to the differences in temperature dependence of the two steps of the solution-precipitation process. Activation energies were found to be 75,000 cal/mole for the solution process and 85,000 cal/mole for the diffusion process. Arrhenius' plots for the three alloy compositions can be found in Figures 5-7.

In Figure 8 linear shrinkage is independent of weight fraction matrix above a minimum matrix content

of 0.125 w/o. Below this matrix content linear shrinkages are lower for comparable sintering cycles. The 0.125 w/o matrix corresponds to a uniform layer of matrix alloy one atom thick on each tungsten particle. This would suggest that, for maximum shrinkage, a continuous interface between tungsten and the matrix alloy is required. However, increasing the depth of the continuous matrix layer has no effect on the shrinkage. Therefore, material transport is not through the bulk matrix, but through the interface between the matrix alloy and the tungsten particle.

Figure 9 shows larger amounts of linear shrinkage with increased nickel fraction in alloys containing a fixed total of 1 w/o copper plus nickel. Copper was added to the nickel to reduce tungsten solubility in the matrix. Although the tungsten-copper-nickel ternary phase diagram is not known, the solubility of tungsten in copper is zero, of tungsten in nickel is 17 a/o, and the solubility of tungsten probably increases with nickel content in copper-nickel alloys. These observations support the theory that increased shrinkage should accompany increased tungsten solubility in the matrix.[4]

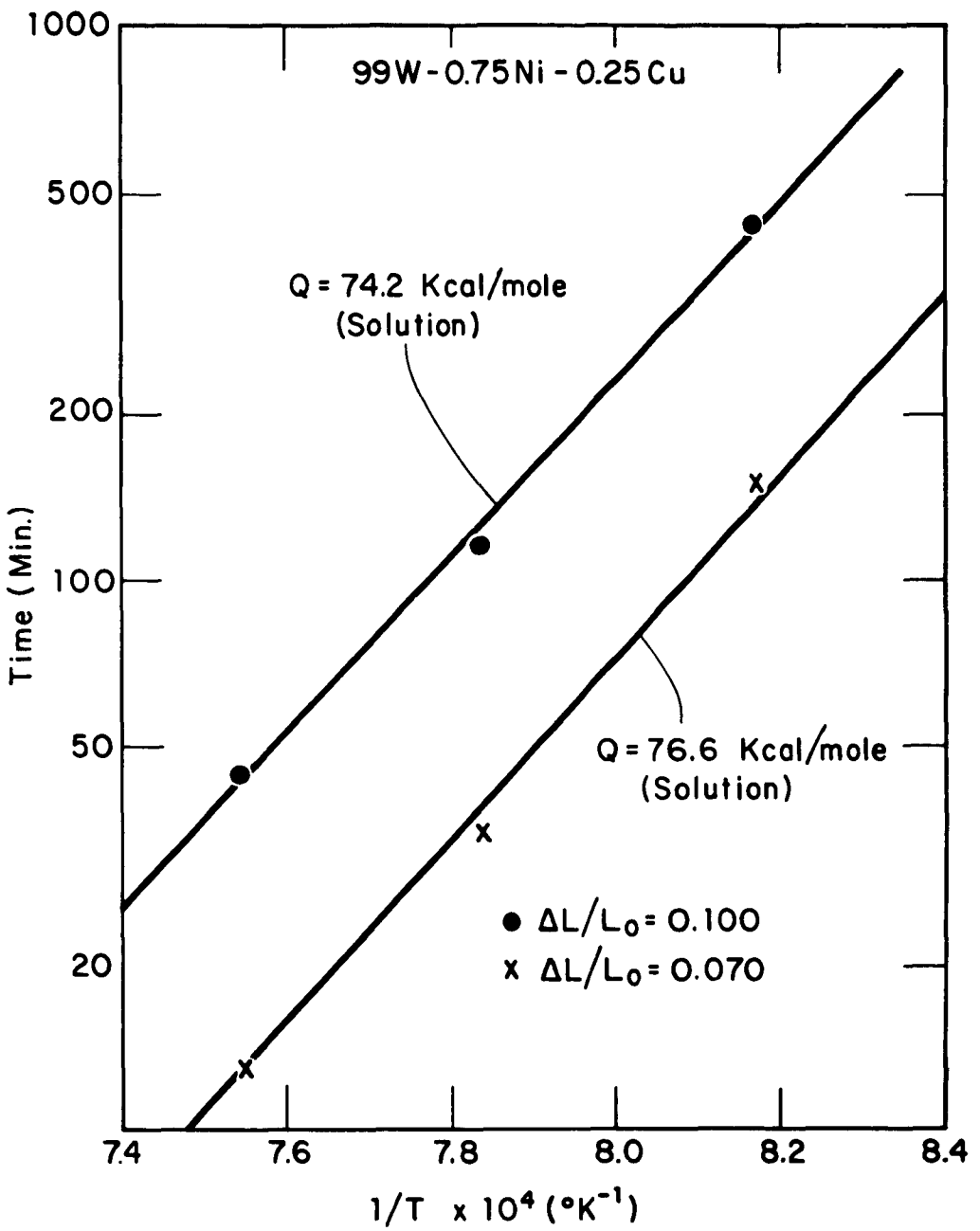

Figure 5: Arrhenius' Plot for 99W-0.75Ni-0.25Cu.

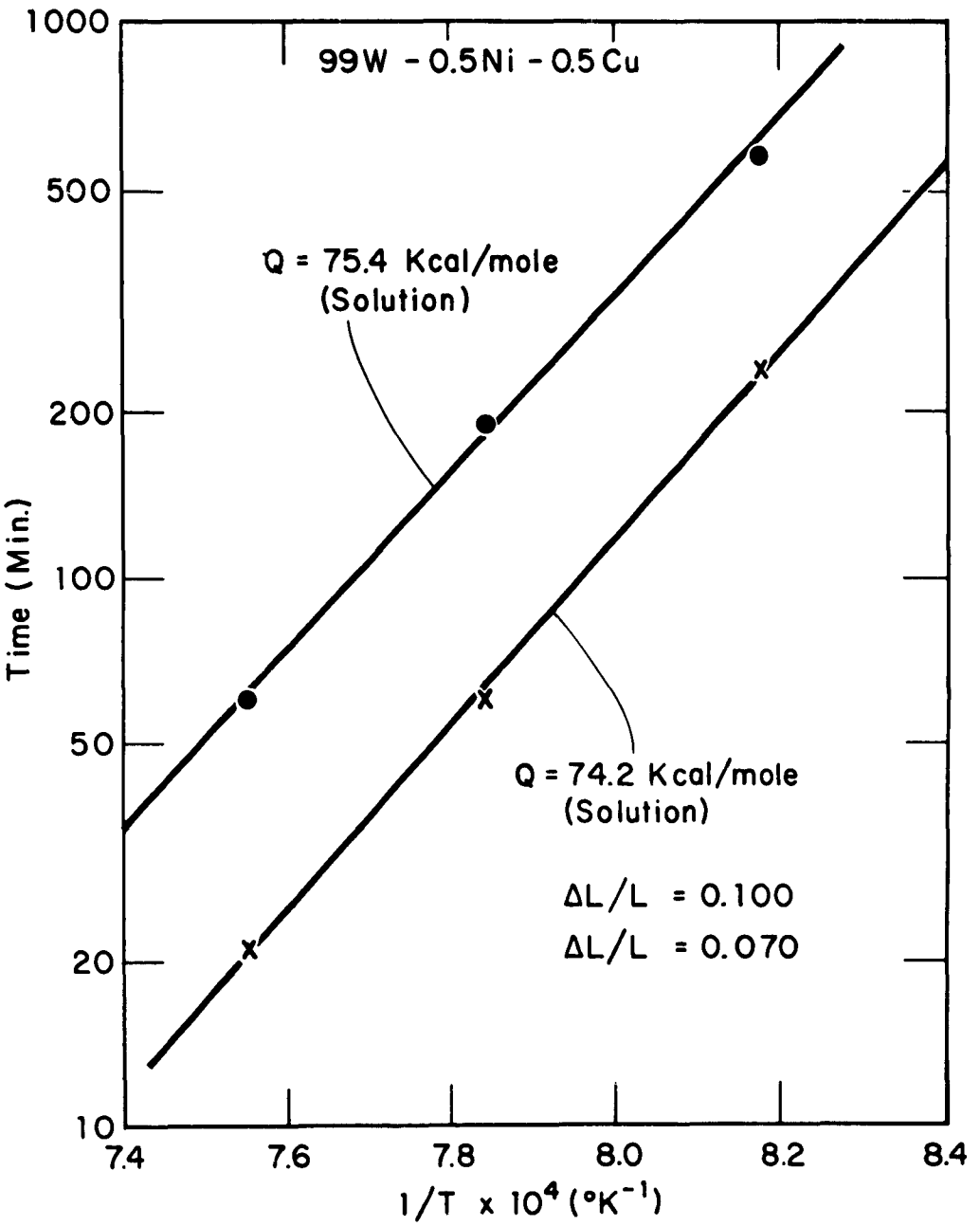

Figure 6: Arrhenius' Plot for 99W-0.50Ni-0.50Cu.

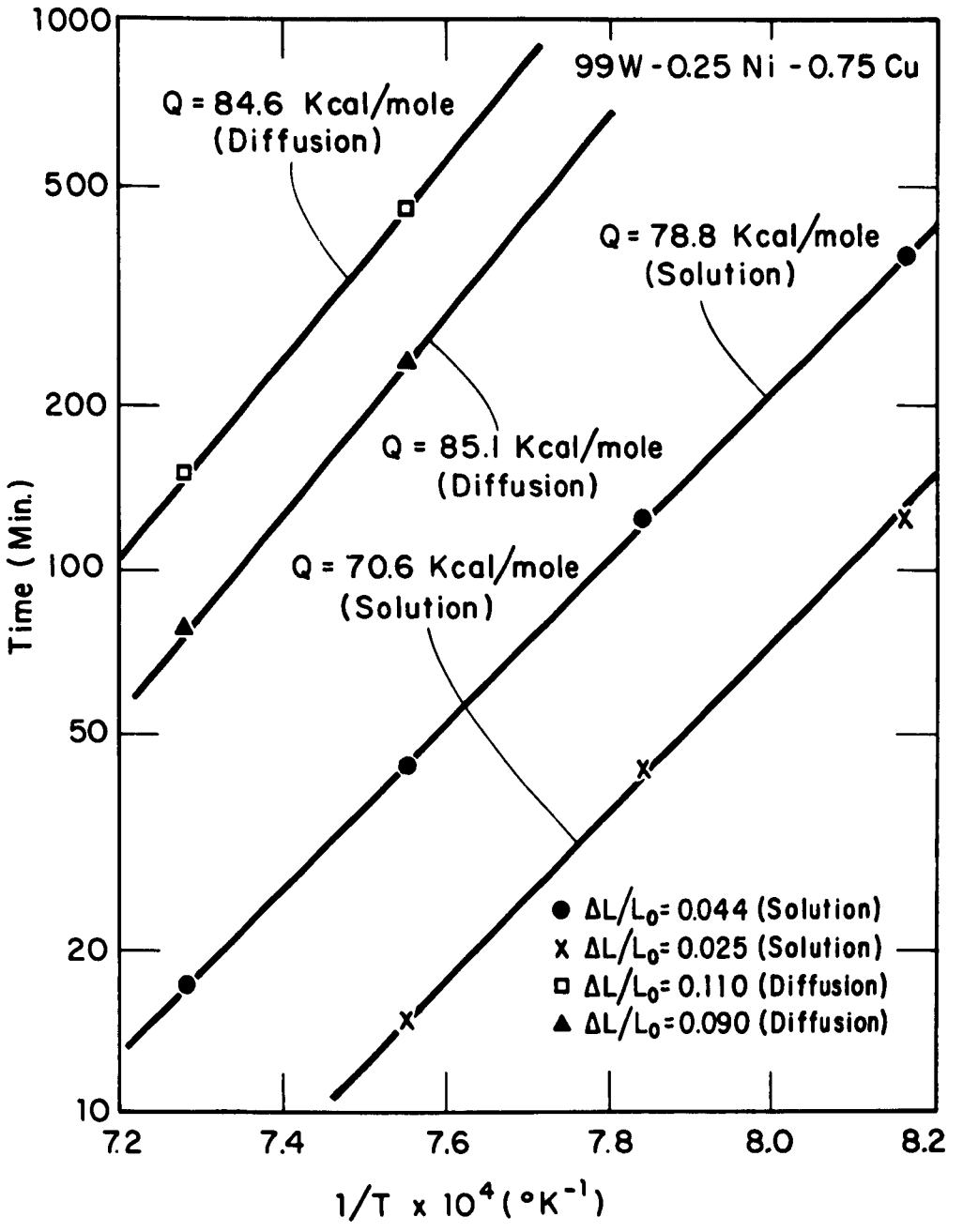

Figure 7: Arrhenius' Plot for 99W-0.25Ni-0.75Cu.

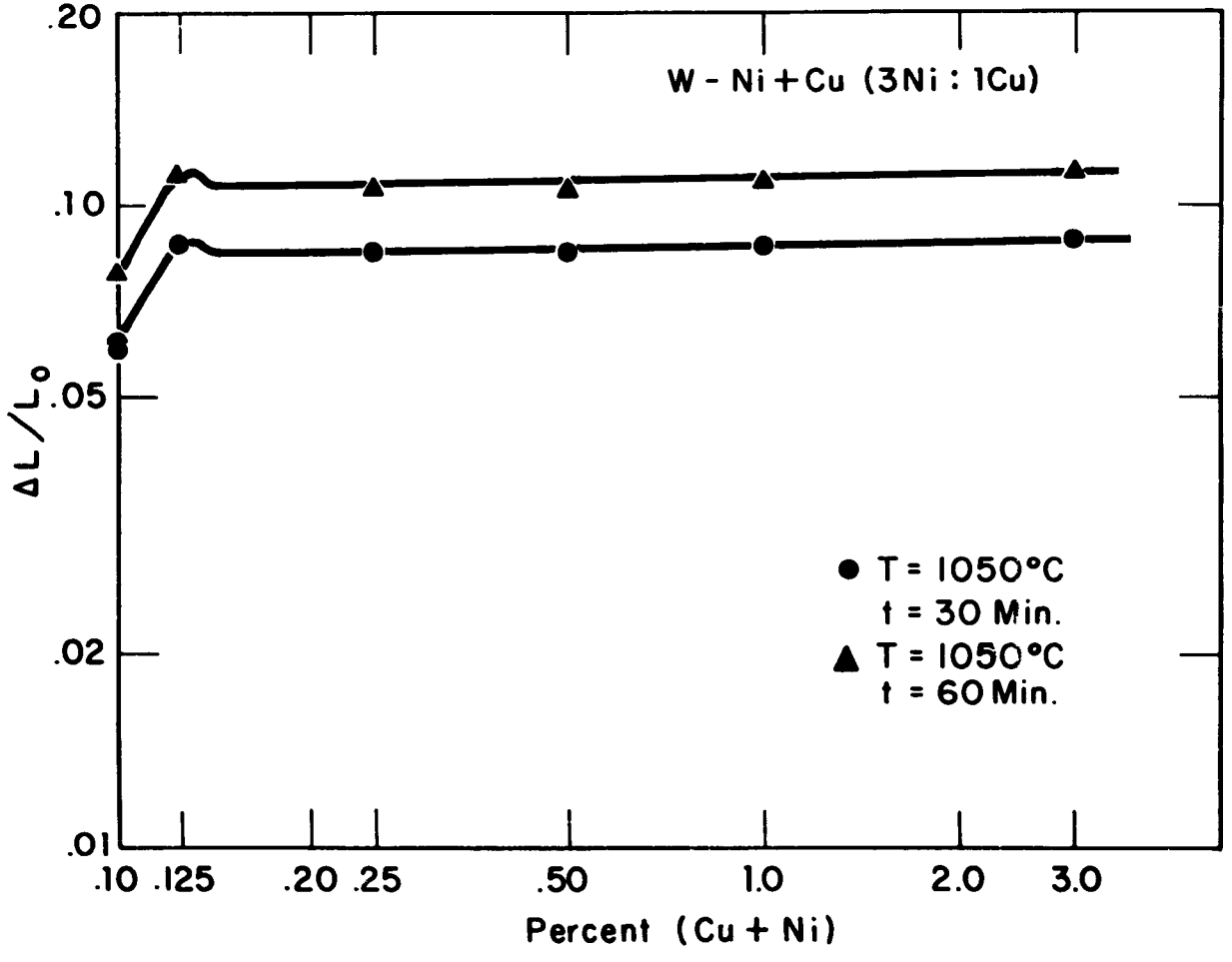

Figure 8: Linear Shrinkage as a Function of Weight Fraction Matrix Alloy for Tungsten-Copper-Nickel Alloys.

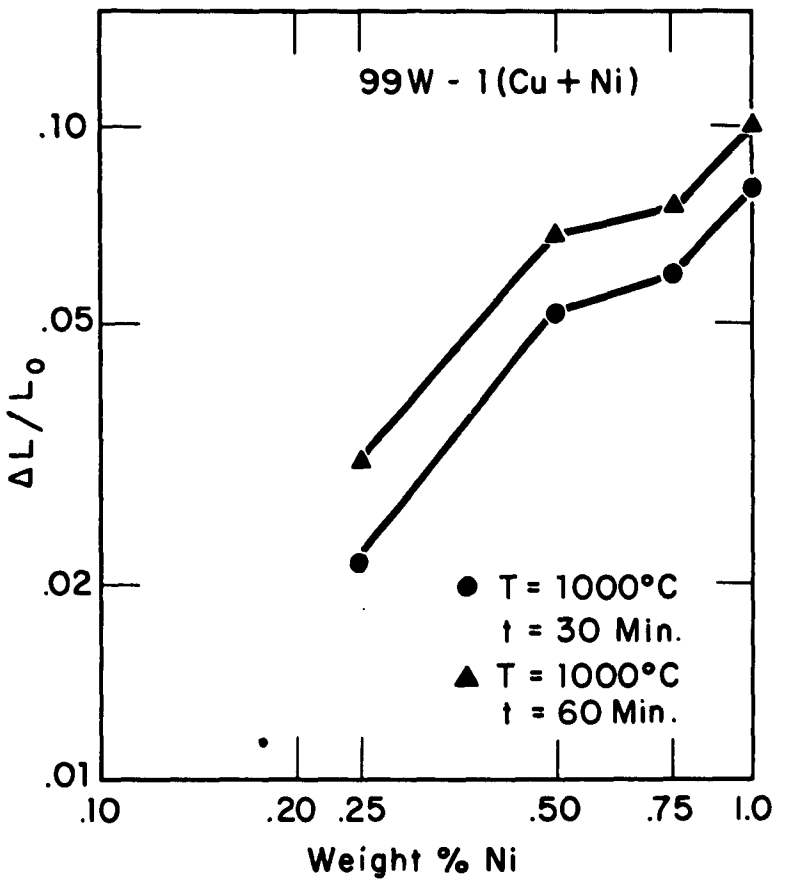

Figure 9: Linear Shrinkage as a Function of Nickel Content for 99W-(Ni+Cu) Alloys.

2) Liquid Carrier Phase Sintering

Alloys of C-20 tungsten powder with 10 w/o additions of 1Ni:1Cu matrix alloy were sintered at 1300-1450°C. The large particle size tungsten (4.07 micron average particle size) was employed to impede the sintering rate and permit the study of the process for reasonable lengths of time. Table II presents the shrinkage data. Figures 10 and 11 are typical liquid phase sintered micro-structures.

Figure 12 is a plot of linear shrinkage versus time, based on the green compact length. However, to analyze the sintering mechanism involved in later stages it is necessary to isolate the shrinkage due to initial rearrangement. Kingery postulated that the amount of rearrangement is proportional to volume fraction liquid only.[7] Since rearrangement is independent of any other process, and happens in a very short period at the beginning of sintering, it is erroneous to analyze linear shrinkage during solution-precipitation on the basis of green length. The magnitude of the error involved increases with the amount of rearrangement which occurs. This is evident from the lower slopes

TABLE II

SHRINKAGE DATA FOR 90W-5.0Ni-5.0Cu ALLOYS SINTERED IN THE LIQUID PHASE

	Time (min.)	Length (in.)	$\Delta L/L_o$	$(\Delta L/L_o)_c$
1300°C	0	2.0050		
	5	1.9645	0.020	-
	10	1.9371	.034	-
	20	1.9034	.051	-
	30	1.8812	.062	-
	45	1.8559	.074	-
	60	1.8373	.084	-
	75	1.8231	.091	-
	100	1.8033	.101	-
1350°C	0	2.0050		
	5	1.8541	.075	0.017
	10	1.8150	.095	.038
	20	1.7776	.113	.058
	30	1.7577	.123	.069
	45	1.7377	.133	.079
	60	1.7250	.140	.086
	90	1.7100	.147	.094
1400°C	0	2.0050		
	5	1.7725	.116	.031
	10	1.7458	.129	.046
	20	1.7252	.140	.057
	30	1.7137	.146	.064
	45	1.7036	.150	.069
	60	1.6980	.153	.072
	90	1.6930	.156	.075
1450°C	0	2.0050		
	5	1.7536	.125	.036
	10	1.7302	.137	.049
	20	1.7106	.147	.060
	30	1.7008	.152	.065

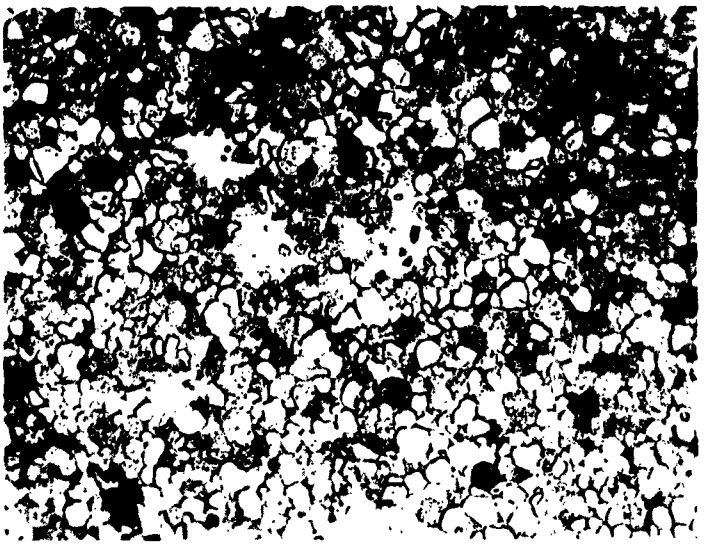

Figure 10: Sample of 90W-5.0Ni-5.0Cu Sintered at 1300°C for 100 Minutes Etched with Wolff's Reagent. 200X

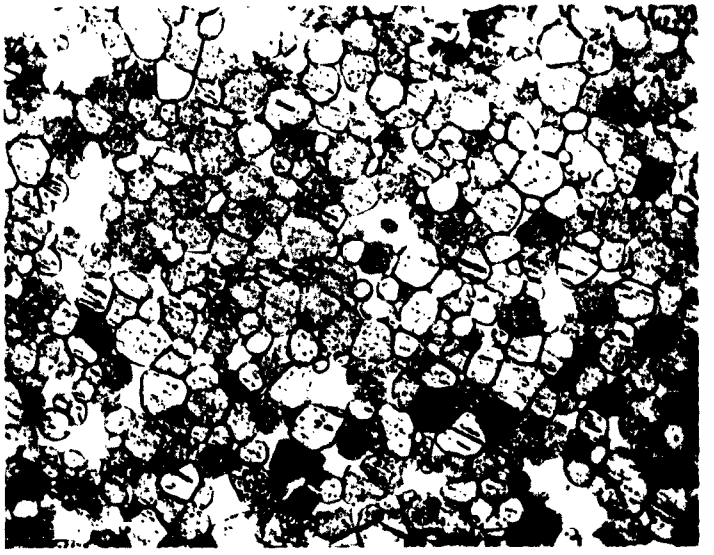

Figure 11: Sample of 90W-5.0Ni-5.0Cu Sintered at 1400°C for 90 Minutes Etched with Wolff's Reagent. 200X

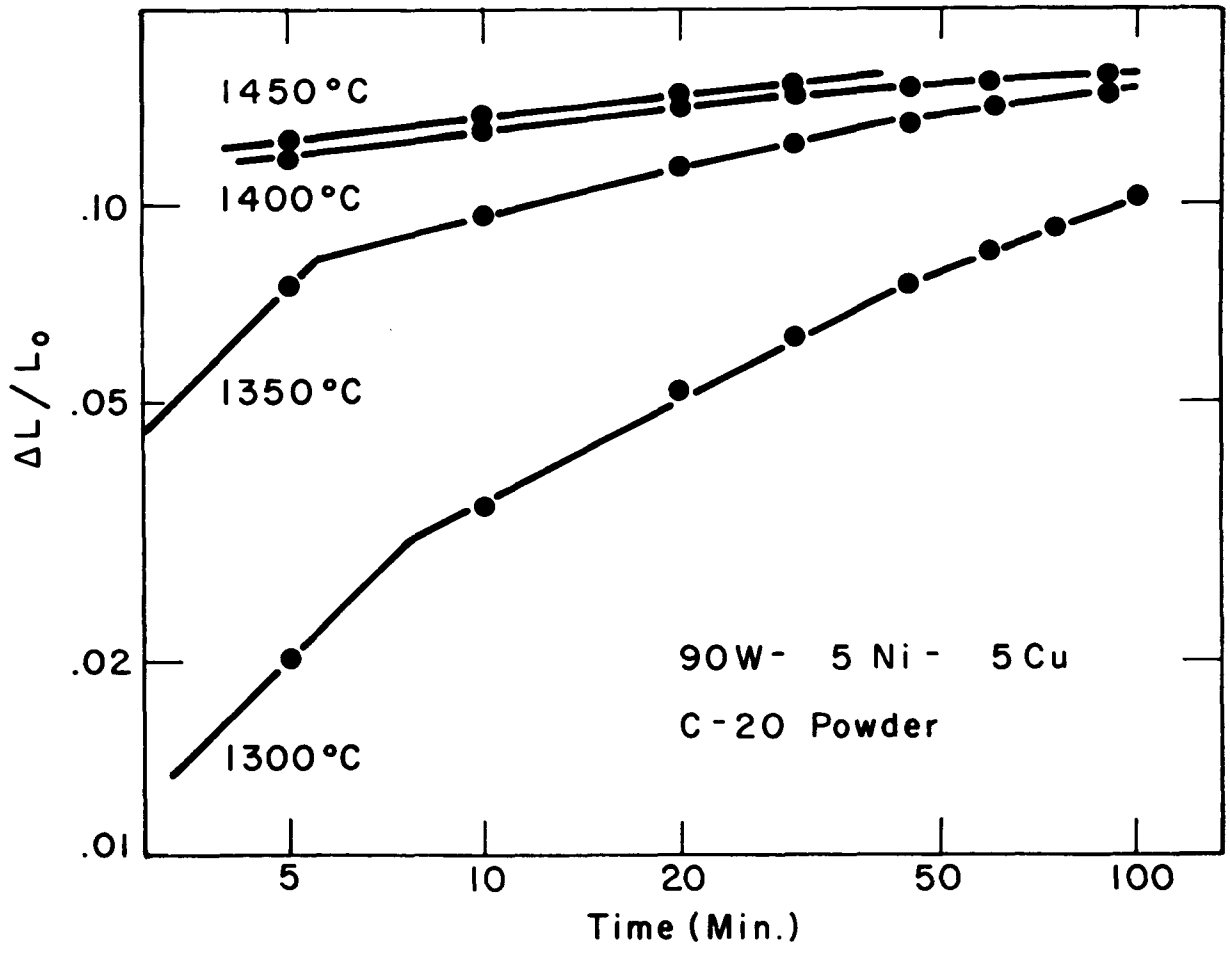

Figure 12: Linear Shrinkage as a Function of Time and Temperature for 90W-5.0Ni-5.0Cu Alloys Sintered with Liquid Phase.

in Figure 12 at higher temperatures, where the amount of rearrangement is greater.

In order to compute the length after rearrangement, the corrected length, $(L_o)_c$, it is necessary to know the amount of liquid phase present at the sintering temperature from the phase diagram. Due to the negligible solubility of tungsten in copper, tungsten does not raise the melting point of copper in the matrix alloy. Tungsten raises the melting point of nickel 40°C. Therefore, it was assumed that tungsten raised the melting point of 1Ni:1Cu matrix alloy by 20°C. This places the liquidus at 1370-1380°C and the solidus at 1290-1300°C. On this basis it was possible to estimate the volume fraction liquid present in 90 w/o tungsten compacts at various temperatures, and the volume change upon "rearrangement"[7].

Recognizing that linear shrinkage due to rearrangement is approximately one-third of volume shrinkage, it is possible to compute corrected initial lengths, $(L_o)_c$, for the solution-precipitation process. Table III is a summary of volume fraction liquid and corrected length as a function of temperature for 90 w/o tungsten alloys with 1Ni:1Cu matrix composition.

Figure 13 is a plot of corrected linear shrinkage versus time. The shrinkage curves all begin with slopes of 1/2, switching to slopes of 1/3 as in the solid phase sintered data of Figures 2-4. This indicates that, after rearrangement, sintering proceeds by the normal solution-precipitation process. In Figure 13 the highest temperature shrinkage plots enter final stage sintering at lowest corrected shrinkage values. This can be attributed to the fact that the onset of final stage sintering is determined by a value of total shrinkage and, when a larger amount of rearrangement has occurred, a smaller amount of solution-precipitation is possible.

It is not possible to compute meaningful activation energies for this process due to the uncertainties introduced by the lack of the phase diagram. Small variations in estimated volume fraction liquid at a given temperature can alter the level of the corrected shrinkage plot which, in turn, alters the calculated activation energy.

TABLE III

VOLUME FRACTION LIQUID AND CORRECTED LENGTH AS A FUNCTION OF TEMPERATURE FOR 90W-5.0Ni-5.0Cu ALLOYS

Temp. (°C)	% Liquid	$(L_o)_c$ (in.)*
1300	none	2.0050
1350	17.0	1.8870
1400	25.5	1.8300
1450	27.0	1.8200

* Green lengths were 2.0050 in. in all cases.

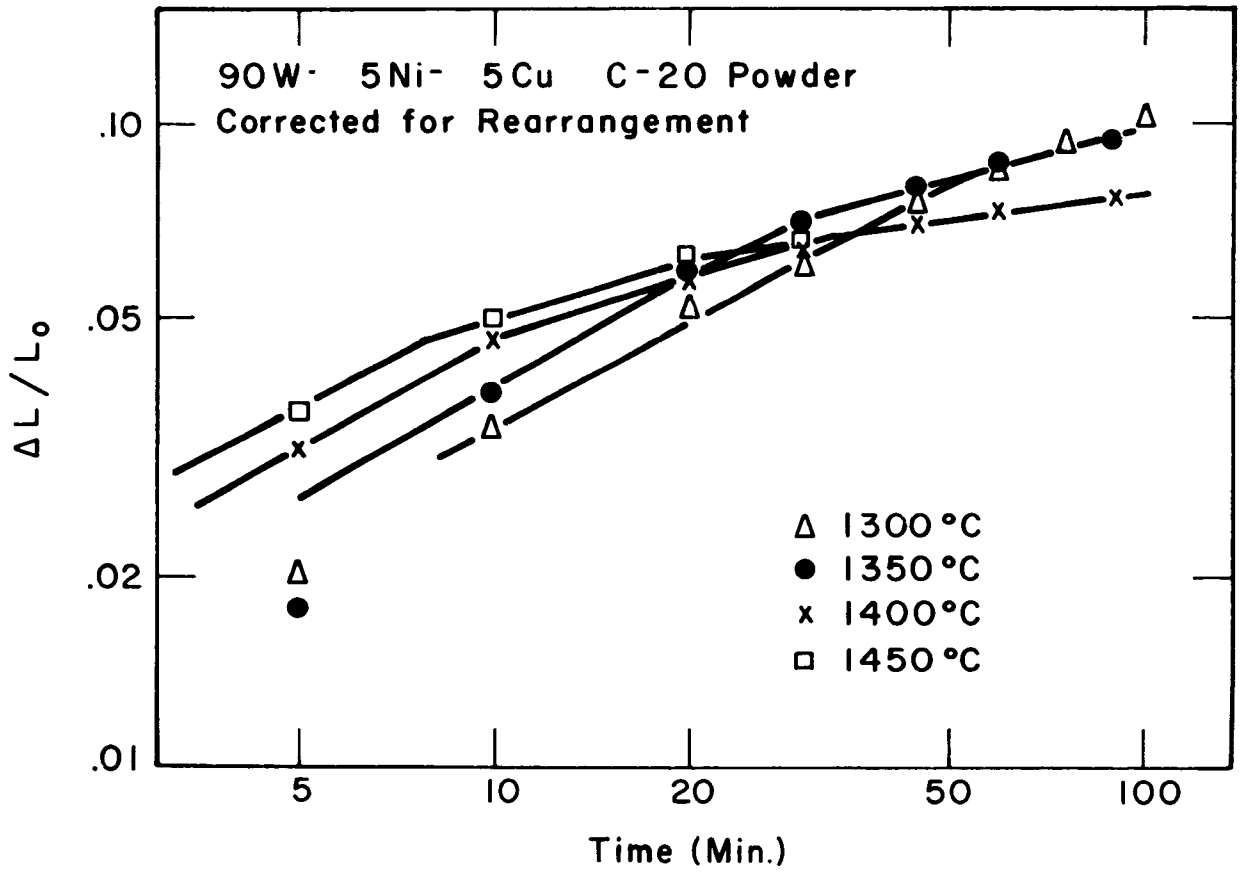

Figure 13: Corrected Linear Shrinkage as a Function of Time and Temperature for 90W-5.0Ni-5.0Cu Alloys Sintered with Liquid Phase.

3) The Transition from Solid to Liquid Carrier Phase Sintering

To examine solid state sintering of the same material investigated in the liquid phase region, a sample of 90 w/o C-20 tungsten with 10 w/o 1Ni:1Cu matrix alloy was sintered below the solidus, at 1250°C. This alloy expanded after 20 minutes at 1250°C and Figure 14 shows its microstructure. Kirkendall porosity can be seen in the matrix phase, and the matrix alloy is not homogeneously distributed in the structure, due to mechanical milling preparation.

In order to eliminate the formation of Kirkendall porosity during sintering in the solid phase, alloys containing only 1 w/o matrix and C-10 tungsten powder were prepared by co-reduction and pre-diffusion of nickel and copper salts. The matrix alloy composition was 3Ni:1Cu. Figures 15 and 16 are plots of linear shrinkage and corrected linear shrinkage versus time respectively. Table IV gives the sintering data. The rapid early densification in Figure 15 at all temperatures indicates a rearrangement process for the solid phase (1300°C and 1350°C) as well as for the liquid phase (1400°C). Kingery attributed the rearrangement process to a mechanical sliding or vis-

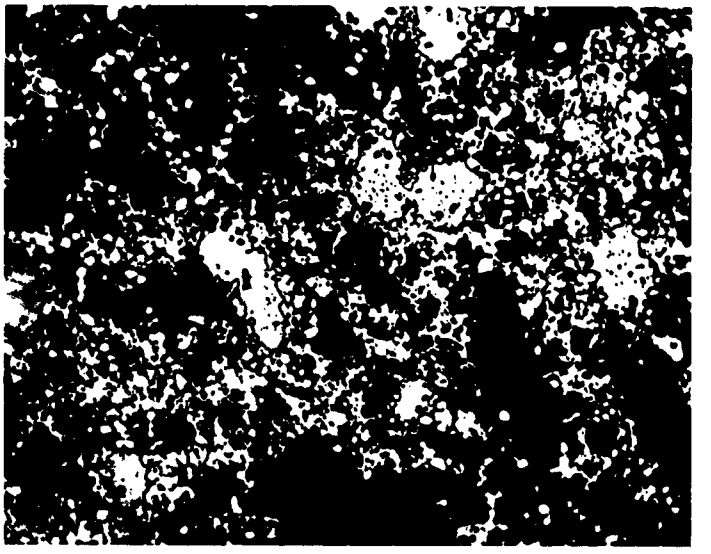

Figure 14: Sample of 90W-5.0Ni-5.0Cu Sintered at 1250°C for 20 Minutes Showing Kirkendall Porosity in the Matrix Alloy Etched with Cold NH_4OH. 500X

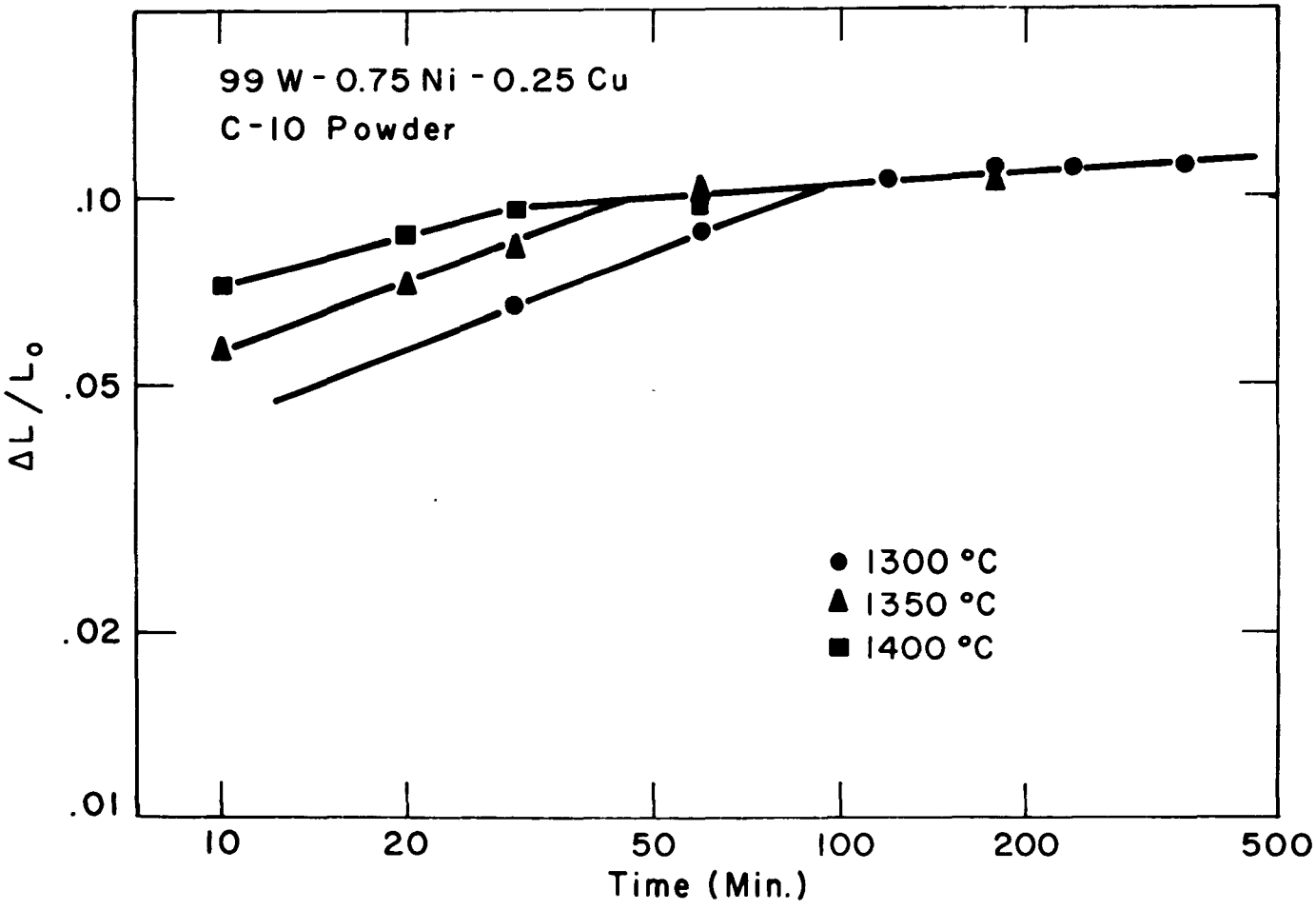

Figure 15: Linear Shrinkage as a Function of Time and Temperature for 99W-0.75Ni-0.25Cu Alloys Sintered in the Temperature Range 1300-1400°C.

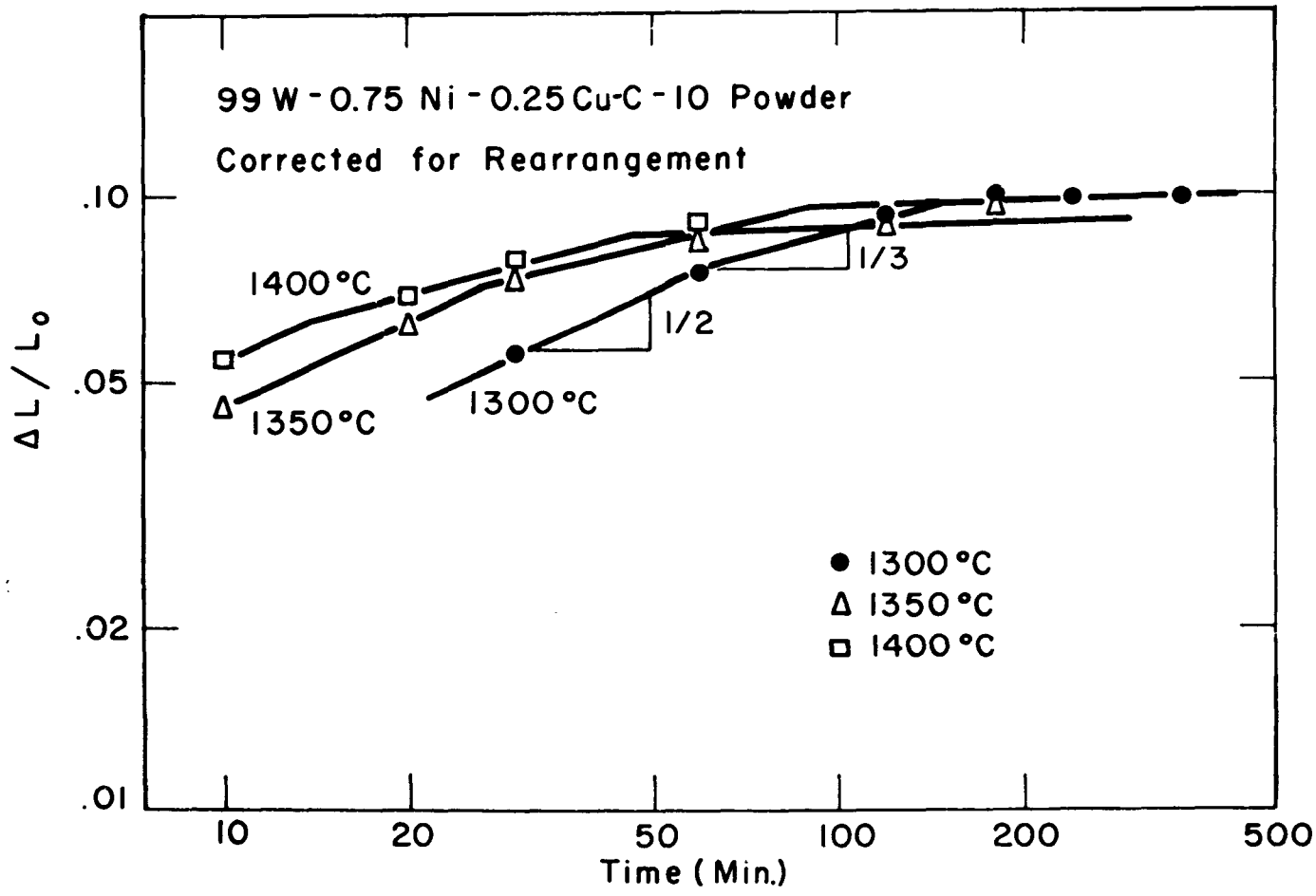

Figure 16: Corrected Linear Shrinkage as a Function of Time and Temperature for 99W-0.75Ni-0.25Cu Alloys Sintered in the Temperature Range 1300-1400°C.

cous flow of solid particles after melting of the matrix phase.[7] Therefore, some rearrangement by particle sliding can also occur when the matrix is solid, if the temperature is sufficiently near the solidus to permit the matrix layer to deform easily. Evidently, the observation of solid state rearrangement is sensitive to the mode of powder preparation. It was not observed in the mechanically mixed powder either because of agglomeration or expansion of the matrix material, while it was observed in co-reduced powders, which are uniformly coated with a thin layer of matrix alloy.

4) Diffusional Porosity

The expansion observed in the heavy metal compositions (10 w/o matrix, balance tungsten) of the preceding section is attributed to diffusional (Kirkendall) porosity, evident in Figure 14. Similar expansions have been frequently observed in the production of sintered alloys.[10-14] In copper-nickel alloys, expansion has been attributed to Kirkendall porosity formed in the solid state.[11,14] In copper-iron and copper-tin alloys, growth has been explained by a form of diffusional porosity

TABLE IV

SHRINKAGE DATA FOR 99W-0.75Ni-0.25Cu ALLOYS

SINTERED IN THE TEMPERATURE RANGE 1300-1400°C

	time (min.)	length (in.)	$\Delta L/L_o$	$(\Delta L/L_o)_c$
1300°C*	0	2.0022		
	30	1.8699	0.066	0.054
	60	1.8313	.085	.073
	120	1.7958	.103	.090
	180	1.7842	.109	.096
	240	1.7813	.110	.097
	360	1.7795	.111	.098
1350 C*	0	2.0021		
	10	1.8881	.057	.045
	20	1.8564	.073	.061
	30	1.8351	.083	.072
	60	1.8063	.098	.086
	180	1.7879	.107	.096
1400°C*	0	2.0018		
	10	1.8590	.071	.054
	20	1.8318	.095	.068
	30	1.8166	.093	.076
	60	1.8013	.100	.084
	120	1.7930	.104	.088

*Corrected initial lengths after rearrangement are 1.9766, 1.9766 and 1.9651 for 1300°C, 1350°C and 1400°C respectively.

involving a liquid-solid diffusion couple (in contrast to the solid-solid couple of the Kirkendall experiments).[10,13]

In this investigation, a corollary study of diffusional porosity was included for two reasons. First, the liquid phase sintering theory of Kingery et al was proposed using evidence of shrinkage in the iron-copper system without encountering the growth mentioned previously.[7,15,16] Second, the Kirkendall effect tended to mask the study of solid state sintering of tungsten-copper-nickel.

Upon sintering of iron-copper alloys an expansion is observed.[10,12,13] This is attributed to the diffusion of copper into the iron. Alloys containing 10 and 20 v/o copper were sintered at 1150°C. To emphasize the kinetic effect two types of iron powder, very fine carbonyl (1 micron average particle size) and coarse Swedish sponge iron (-100 mesh) were used. The very fine carbonyl powder mix sintered to full density in less than 10 minutes, while the Swedish iron powder mix expanded greatly before shrinking at a low rate. With increased copper content the tendency toward shrinkage was greater due to the increased amount of liquid phase present after full diffusion of copper

into the iron. Since the copper powder was the same in both cases it can be assumed that copper diffusion into the iron was achieved at the same rate in all cases. Therefore, the tendency for the carbonyl iron to shrink while the sponge iron expands can be explained by the differences in iron particle size. In the case of carbonyl iron, solution-precipitation sintering occurred at such a rapid rate that the expansion due to copper diffusion was negligible compared to short time shrinkage. However, shrinkages after short time sintering of Swedish iron powder by the solution-precipitation process were so small, due to the large particle size, that expansion predominated.

A heavy metal specimen containing 10 w/o copper-nickel expanded upon sintering for short times at 1250°C. See Figure 14 for the microstructure. This expansion would seem counter to theory, since the melting point of copper is 1083°C. Sintering of compacts of the matrix alloy alone for short periods at 1150°C resulted in even more impressive expansions. These results can be attributed to the fact that interdiffusion of nickel and copper occurs extremely rapidly at temperatures in excess of 1000°C. Therefore,

it is logical to assume that homogenization, resulting in expansion, occurs before the melting point of copper is reached. The homogeneous alloy has a melting point above 1250°C, resulting in no melting. Therefore, the porosity is stable.[11] It was found that the amount of expansion observed in copper-nickel matrix alloys (without tungsten) increased with increased in either copper or nickel particle sizes. Table V is a summary of the expansion data.

In systems which exhibit an expansion effect, densification during sintering can mask the expansion completely. Alloys containing 90 w/o tungsten, sintered in the solid phase, shrink immediately if C-5 tungsten powder is used, but expand before beginning to shrink if C-20 powder is employed. The analysis is kinetic in nature. Small tungsten powders sinter more rapidly by solution-precipitation than do large powders. Therefore, expansion predominates for large particle sized powders, while the reverse is true for small tungsten powders.

TABLE V

KIRKENDALL EXPANSION AS A FUNCTION OF COPPER AND NICKEL PARTICLE SIZE IN 50Ni-50Ni-50Cu ALLOYS

Cu mesh	Ni mesh	L_o (in.)	L (in.)	$\Delta L/L_o$
-150	-150	2.0009	2.0920	0.046*
-325	-150	2.0014	2.0166	0.0076*
-150	-325	2.0015	1.9678	-0.017*
-325	-325	2.0017	1.9143	-0.044*

* signifies expansion and - denotes shrinkage

CONCLUSIONS

1) Tungsten-copper-nickel alloys sinter by a solution-precipitation process. Activation energies in the temperature range 900-1100 C (solid phase) are 75,000 cal/mole for solution of tungsten and 85,000 cal/mole for diffusion of tungsten out from the line of interparticle centers.

2) Linear shrinkage for tungsten-copper-nickel alloy compositions at contant time, temperature and tungsten particle size increases with increasing tungsten solubility (decreasing weight fraction copper) in the matrix carrier phase.

3) Linear shrinkage is independent of weight fraction matrix above a minimum matrix content of 0.125 w/o. Below this content linear shrinkages for comparable sintering treatments are lower.

4) Plots of corrected linear shrinkage (due to solution-precipitation alone) versus time can be obtained by eliminating the effect of initial re-arrangement shrinkage on measured lengths during sintering. The corrected plots are all composed of segments of 1/2 and 1/3, consistent with the solution-precipitation process.

5) Solid phase rearrangement can occur at temperatures which are high enough to permit easy deformation of the homogeneously deposited, co-reduced matrix alloy. This rearrangement may be a function of powder preparation, since it is not observed in milled powders because of either the agglomerated state of the matrix alloy or the Kirkendall porosity which forms early in sintering.

6) The same mechanisms of sintering predominate in both liquid and solid phase sintering of tungsten-copper-nickel alloys, indicating that both are special cases of the carrier phase sintering process.

7) Diffusional porosity occurs in the matrix alloy of tungsten-copper-nickel compacts. If the matrix does not melt, it can mask any tendency toward shrinkage due to solution-precipitation, particularly with large tungsten particle size, when the solution-precipitation process is slow.

8) Copper-iron compacts, sintered above the melting point of copper, swell due to diffusion of copper into solid iron if large particle size iron powders are used. Very small iron powders produce immediate and rapid shrinkage, due to more rapid solution-precipitation with decreasing iron particle size.

BIBLIOGRAPHY

1. M. Pirani, "Early Days of Nickel-Tungsten Powder Metallurgy," J. Electrochemical Soc., 85 (1944), p. 163.

2. G.H.S. Price, C.J. Smithells, S.V. Williams, "Sintered Alloys Part I- Copper-Nickel-Tungsten Alloys Sintered With A Liquid Phase Present," J. Inst. of Metals, 62 (1938) p. 239.

3. J. Vacek, "On Influencing the Sintering Behavior of Tungsten," Planseeberichte fur Pulvermetallurgie, 7, (1959) p. 6.

4. J.H. Brophy, L.A. Shepard, J. Wulff, "Nickel Activated Sintering of Tungsten," Powder Metallurgy, ed. by W. Leszynski, AIME, MPI, Interscience, New York (1961) p. 113.

5. H.W. Hayden, "Nickel Activated Sintering of Tungsten," B.S. Thesis, Metallurgy Department, M.I.T., 1960.

6. H.W. Hayden, J.H. Brophy, "The Activated Sintering of Tungsten with Group VIII Elements," submitted for publication.

7. W.D. Kingery, "Densification During Sintering in the Presence of a Liquid Phase, I. Theory," J. App. Phys., 30 (1959) #3, p. 301.

8. R.L. Coble, "Diffusion Sintering in the Solid State," Kinetics of High Temperature Processes, ed. by W.D. Kingery, Tech Press-Wiley (1959), p. 147.

9. H.W. Hayden, J.H. Brophy, "Grain Boundary Diffusion in Tungsten Sintering," submitted for publication.

10. G. Matsumura, "Swelling in Iron-Copper Compacts During Sintering," Planseeberichte fur Pulvermetallurgie, 9 (1961), p. 33.

11. B. Fisher, P.S. Rudman, "Kirkendall Effect Expansion During Sintering in Cu-Ni Compacts," Acta Met., 10 (1962), p. 37.

12. W.D. Jones, Fundamental Principles of Powder Metallurgy, Edward Arnold Ltd., London (1960) p. 476.

13. J.E. Elliott, "Growth of Sintered Metal Compacts," Metallurgia, Jan., 1959 p. 17.

14. G.C. Kuczynski, P. Stablein, Unpublished Report to International Nickel Co. (1958).

15. W.D. Kingery, M.D. Narasihman, "Densification During Sintering in the Presence of a Liquid Phase, II. Experiment," J. App. Phys., 30 (1959) #3, p. 307.

16. W.D. Kingery, E. Niki, M.D. Narasihman, "Sintering of Oxide and Metal Composites in the Presence of a Liquid Phase," J. Amer. Cer. Soc., 44 (1961), p. 29.

DISTRIBUTION LIST

Contract No. NOas 61-0326-d

1. Naval Air Material Center
   Philadelphia 12, Pa.
   ATTN: Aeronautical Materials Laboratory

2. Bureau of Ships, Navy Dept.
   Washington 25, D. C.
   ATTN: Codes 347 and 1500

3. Office of Naval Research
   Department of the Navy
   Washington 25, D. C.
   ATTN: Code 423

4. Naval Research Laboratory
   Washington 25, D. C.

5. Watertown Arsenal Lab.
   Watertown, Massachusetts
   ATTN: Mr. Norman Reed

6. Wright Air Development Div.
   Wright-Patterson Air Force Base, Ohio
   ATTN: WCLT, WCREE

7. U.S. Naval Weapons Plant
   Washington 25, D. C.

8. National Aeronautics and Space Administration
   1512 H Street, N. W.
   Washington 25, D.C.(6 copies)

9. A.E.C., Research Division
   Germantown, Maryland

10. Office of Ordnance Res.
    Box CM, Duke Station
    Durham, N. C.

11. Army Ballistic Missile Agency
    Huntsville, Alabama
    ATTN: Mr. W.A. Wilson, ORDAS, DFP

12. Flight Propulsion Lab.Dept.
    General Electric Company
    Cincinnati 15, Ohio
    ATTN: Mr. M.A. Levinstein

13. United Aircraft Corp.
    Pratt & Whitney Div.
    East Hartford, Conn.

14. Space Technology Labs.
    P. O. Box 95001
    Los Angeles, California
    ATTN: Mr. V.J. Tronolone

15. Stanford Research Institute
    Menlo Park, California
    ATTN: Mr. Jess W. Wilson
    Metallurgist,Bldg.106

16. Vitro Laboratories
    200 Pleasant Valley Way
    West Orange, N. J.
    ATTN: Mr. L.C. Terminello

17. Aerojet-General Corp.
    Sacramento, California
    ATTN: Mr. R.A. Perkins

18. Armour Research Foundation
Technology Center
Chicago 16, Illinois

19. General Motors Corp.
Allison Division
Indianapolis, Indiana
ATTN: Mr. D.K. Hanink

20. Curtiss Wright Corp.
Wright Aeronautical Div.
Wood Ridge, N. J.
ATTN: Mr. A. Slachta

21. Thompson Ramo Woodridge, Inc.
23555 Euclid Avenue
Cleveland 17, Ohio
ATTN: Mr. G.N. Guarnieri
Staff R and D

22. National Research Corp.
70 Memorial Drive
Cambridge 42, Mass.
ATTN: Mr. J. H. Gardner

23. Battelle Memorial Institute
505 King Avenue
Columbus 1, Ohio
ATTN: Defense Metals Inf. Center

24. Denver Research Institute
University Park
Denver 10, Colorado
ATTN: Dr. J.P. Blackledge

25. Southern Research Institute
917 S. 20th Street
Birmingham, Alabama
ATTN: Mr. E. J. Wheelahan

26. Westinghouse Electric Co.
Metals Plant
Blairsville, Pa.
ATTN: Mr. J.C. McClure

27. Aerospace Industries Asso.
610 Shoneham Building
Washington 5, D. C.
ATTN: Mr. Jack Reese,
Technical Service
(3 copies)

28. Wright Air Development Div.
Wright-Patterson Air Force
Base, Ohio
ATTN: Lawrence N. Hjelm,
2/Lt. USAF
Exploratory Applications
Section
Design Criteria Branch
Applications Division